Hadronic spectrum in the chiral large N_c extension of quantum chromodynamics

Axel Halgaard Kristensen* and Thomas A. Ryttov†

CP[3] *-Origins, University of Southern Denmark, Campusvej 55, 5230 Odense M, Denmark*

(Received 23 April 2024; accepted 7 June 2024; published 9 July 2024)

We study quantum chromodynamics in the chiral large N_c limit which contains a left-handed Weyl fermion in the fundamental representation, a left-handed Weyl fermion in the two index antisymmetric representation and $(N_c - 3)$ left-handed Weyl fermions in the antifundamental representation of the $SU(N_c)$ gauge group. We construct gauge singlet composite operators and study their masses and correlation functions at large N_c. It is shown that all hadron masses scale as $\sim N_c^0 n_q$ where n_q is the number of constituent quarks in the hadron. In addition by simple gluon exchange considerations it is seen that scattering amplitudes between hadrons have the same N_c scaling as the mass of the lightest hadron involved. This is the case provided the hadrons in the scattering amplitude share a sufficiently large number of constituent quarks. The chiral large N_c extension also allows for other nontrivial processes. For instance we consider two different baryonium states that are unique to this extension and that decay via emissions of two- and three-quark hadrons. Also other nontrivial scattering processes are considered. Finally, we study composites made of a mix of left- and right-handed fields. We categorize multiple groups of hadrons within the full spectrum according to their flavor structure. Within these groups all n-point functions scale the same.

DOI: 10.1103/PhysRevD.110.014012

I. INTRODUCTION

The strong interactions of quarks and gluons continue to be one of the most difficult phenomena to understand even more than 50 years after the birth of quantum chromodynamics (QCD) [1–4]. Great effort has been put into understanding the spectrum and physics at low and intermediate energies using lattice simulations [5,6], higher order perturbation theory which is currently known to five loops [7,8] for the running of the gauge coupling, large N_c techniques [9,10], holography and light cone quantization [11,12]. The literature is immense but a few recent reviews on several aspects of QCD can be found here [13–15].

In this work we are particularly interested in studying QCD in a large number of colors N_c approach. In QCD with $N_c = 3$ the quarks are in the fundamental representation of the $SU(N_c = 3)$ gauge group. In the original large N_c extension of QCD [9,10,16–19] the quarks are kept in the fundamental representation of the $SU(N_c)$ gauge group. We will refer to this extension as the 't Hooft limit. At infinite N_c there are a number of simplifications such as the suppression of nonplanar diagrams and quark loops. On the other hand it also adds a complication since baryons contain N_c quarks and therefore an infinite product of quarks at infinite N_c.

Another extension is to consider the 't Hooft limit but with N_f pairs of fundamental quarks and then taking the large N_f limit with N_f/N_c kept fixed [20,21]. We will refer to this as the Veneziano limit. This limit is used in [22–25] in a holographic approach to QCD.

At $N_c = 3$ the two index antisymmetric representation is equivalent to the antifundamental representation. So to remedy the baryon problem just mentioned, Corrigan and Ramond proposed to add a quark in the two index antisymmetric representation in addition to the fundamental quarks [26–30]. As one extends QCD to large N_c one can then form a baryon containing only three quarks at any N_c. We will refer to this extension as the Corrigan-Ramond extension. If the quarks belong to the two index antisymmetric representation then the quark loops are not suppressed at infinite N_c and are on an equal footing with the gluons in terms of counting of the number of degrees of freedom.

Now it is also possible to consider having only two index antisymmetric quarks and no fundamental quarks at any N_c [31–34]. At $N_c = 3$ this is still ordinary QCD. We will refer to this extension of QCD as the orientifold limit. If we consider a single quark in the two index antisymmetric representation at infinite N_c this extension shares parts of

*Contact author: axkri19@student.sdu.dk
†Contact author: ryttov@cp3.sdu.dk

its bosonic sector with $\mathcal{N} = 1$ supersymmetric Yang-Mills theory [35–39].

In this work we consider a large N_c extension of QCD first proposed in [40] that in a certain sense stands in between the 't Hooft and orientifold large N_c limits and simultaneously share certain features with the Veneziano limit. It does so in a nontrivial way since it is a chiral extension of $SU(N_c = 3)$ QCD and one has to be careful about possible gauge anomalies. It is in this little honey hole between the above mentioned time honored large N_c extensions our investigations will unfold. Our results are complementary to the results derived in the past for the various large N_c limits.

The work is organized as follows. In Sec. II we introduce the large N_c chiral extension of QCD, in Sec. III we comment on a number of different properties of the chiral extension and in Sec. IV we give a brief review of large N_c counting techniques. In Sec. V we provide a detailed analysis of the composite spectrum, their masses and various interactions. We finally end with the conclusions in VI.

II. THE CHIRAL LARGE N_c EXTENSION

The chiral large N_c extension is a third limit of QCD which in some sense is in between the 't Hooft and orientifold limits. Schematically it can be seen in Fig. 1 which is taken from [40]. In the chiral large N_c limit we consider a gauge theory with gauge group $SU(N_c)$ and with associated gauge fields $(A_\mu)^i_j$ in the adjoint representation where $\mu = 0, \ldots, 3$ is a Lorentz index and $i, j = 1, \ldots, N_c$ are $SU(N_c)$ gauge indices. We also add a single left-handed Weyl fermion q^i_α in the fundamental representation of the gauge group and a single left-handed Weyl fermion $\tilde{q}^{[ij]}_\alpha = -\tilde{q}^{[ji]}_\alpha$ in the two index antisymmetric representation of the gauge group. This is a chiral gauge theory, and in order to cancel the gauge anomaly we add $(N_c - 3)$ left-handed Weyl fermions $Q_{\alpha,i,f}$ in the antifundamental representation of the gauge group. Here the index α is an $SL(2,\mathbb{C})$ spinor index and f is a global $SU(N_c - 3)$ index. We will refer to f as a flavor index. The theory is a

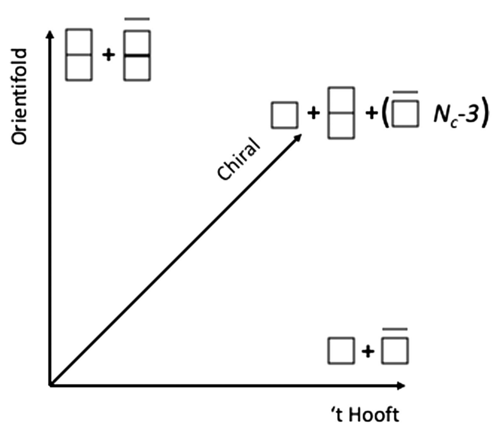

FIG. 1. The three different large N_c limits of QCD.

TABLE I. This table summarizes the particle content of the chiral extension, and shows the charges of the two anomaly free $U(1)$ symmetries.

	$[SU(N_c)]$	$SU(N_c-3)$	$U_1(1)$	$U_2(1)$
q_α	$\square$	1	$N_c - 2$	$-(N_c - 1)$
$\tilde{q}_\alpha$	$\begin{smallmatrix}\square\\\square\end{smallmatrix}$	1	$N_c - 4$	2
Q_α	$\overline{\square}$	$\overline{\square}$	$-(N_c - 2)$	-1
A_μ	adj	1	0	0

generalized Georgi-Glashow model [41] and is chiral for $N_c > 3$. We here summarize the particle content

The two Abelian $U(1)$ symmetries are both anomaly-free[1]

$$U_1(1){:}\ \ \frac{1}{2}(N_c - 2) + \frac{N_c - 2}{2}2 - \frac{1}{2}(N_c - 2)(N_c - 3) = 0 \tag{1}$$

$$U_2(1){:}\ \ -\frac{1}{2}(N_c - 1) + \frac{N_c - 2}{2}2 - \frac{1}{2}(N_c - 3) = 0 \tag{2}$$

Most importantly for $N_c = 3$ the Weyl fermions $Q_{\alpha,i,f}$ disappear from the spectrum and the two index antisymmetric representation is equivalent to the antifundamental representation. Therefore the theory is vectorlike and is $SU(N_c = 3)$ QCD with a single massless Dirac quark flavor

$$\Psi_D = \begin{pmatrix} q^i_\alpha \\ \epsilon^{ijk}\epsilon^{\dot{\alpha}\dot{\beta}}\bar{\tilde{q}}_{\dot{\beta},[jk]} \end{pmatrix} \tag{3}$$

Our convention for Hermitian conjugation is

$$(\tilde{q}^{[ij]}_\alpha)^\dagger = \bar{\tilde{q}}_{\dot{\alpha},[ij]} \tag{4}$$

The model above provides a third alternative large N_c limit for one flavor QCD. First note that it partly resembles the 't Hooft limit since it contains a Weyl fermion q^i_α in the fundamental representation of the gauge group. Second note that it partly resembles the orientifold limit since it contains a Weyl fermion $\tilde{q}^{[ij]}_\alpha$ in the two index antisymmetric representation of the gauge group. In this sense the large N_c limit we are considering stands in between these two time honored limits. Now third note that to nontrivially cancel the gauge anomalies we add $N_c - 3$ Weyl fermions in the antifundamental representation. Taking the large N_c limit of these fermions then in some sense resembles the Veneziano limit where one takes the limit of a large number of flavors. As a final remark please note that we can trivially extend the large N_c limit of one flavor QCD to that of N_f

[1] The contribution from n left-handed Weyl fermions to a $U(1)$ anomaly is $T_r Q n$ where T_r is the trace normalization factor of the gauge group representation r and Q is the $U(1)$ charge.

flavor QCD by just adding N_f copies of the same fermion content.

Various possible candidate phases for generalized Georgi-Glashow models have been studied in [42]. In general the phase structure of chiral gauge theories has been of significant interest in the past. See for instance [40,43–55].

When taking the large N_c limit we must be careful and make sure that we correctly normalize the fields and properly account for various $SU(N_c)$ color factors. We want to use the double line notation and hence we consider the gauge fields and the Weyl fermions in the two index antisymmetric representation as rank-2 tensor representations. We here summarize our conventions for the generators T_r^a, $a=1,\ldots,N_c^2-1$ the trace-normalization factors T_r, quadratic Casimirs C_r and dimensions d_r for the representation r

$$(T_F)^i{}_j \qquad T_F=\frac{1}{2} \qquad C_F=\frac{N_c^2-1}{2N_c}. \qquad d_F=N_c \tag{5}$$

$$(T_{\bar{F}})_i{}^j=-(T_F^{a*})_i{}^j \quad T_{\bar{F}}=\frac{1}{2} \quad C_{\bar{F}}=\frac{N_c^2-1}{2N_c}. \quad d_{\bar{F}}=N_c \tag{6}$$

$$(T_A^b)^{ac}=if^{abc} \quad T_A=N_c \quad C_A=N_c \quad d_A=N_c^2-1 \tag{7}$$

$$(T_{2A}^a)^{rs}=4\mathrm{Tr}\,A^rT_F^aA^s \quad T_{2A}=\frac{N_c-2}{2}$$
$$C_{2A}=\frac{(N_c+1)(N_c-2)}{N_c} \quad d_{2A}=\frac{N_c(N_c-1)}{2} \tag{8}$$

We also need the following two important identities (completeness relations)

$$(T_F^a)^i{}_j(T_F^a)^k{}_l=\frac{1}{2}\left(\delta^i{}_l\delta^k{}_j-\frac{1}{N_c}\delta^i{}_j\delta^k{}_l\right) \tag{9}$$

$$(A^r)^{ij}(A^r)^{kl}=\frac{1}{4}(\delta^{il}\delta^{jk}-\delta^{ik}\delta^{jl}) \tag{10}$$

where $(A^r)^{ij}$ is a set of linearly independent $N_c\times N_c$ matrices $(A^r)^T=-A^r$. There are $N_c(N_c-1)/2$ such matrices, so $r=1,\ldots,N_c(N_c-1)/2$ [56,57]. We also want to rescale the fields so that the gauge coupling only appears as an overall factor in the Lagrangian. We discuss this in detail in appendix. With these conventions the Lagrangian is

$$\mathcal{L}=\frac{N_c}{\lambda}\left[-\frac{1}{2}\mathrm{Tr}F_{\mu\nu}F^{\mu\nu}+i\bar{q}\bar{\sigma}^\mu D_\mu q+2i\mathrm{Tr}(\bar{\tilde{q}}\bar{\sigma}^\mu D_\mu\tilde{q}) + i\bar{Q}\bar{\sigma}^\mu D_\mu Q-\frac{1}{\xi}\mathrm{Tr}(\partial^\mu A_\mu)^2+2\mathrm{Tr}\bar{c}(-\partial^\mu D_\mu c)\right] \tag{11}$$

with

$$F_{\mu\nu}=F_{\mu\nu}^aT_F^a=\partial_\mu A_\nu-\partial_\nu A_\mu-i[A_\mu,A_\nu] \tag{12}$$

$$D_\mu q^i=\partial_\mu q^i-i(A_\mu)^i{}_jq^j, \qquad (A_\mu)^i{}_j=A_\mu^a(T_F^a)^i{}_j \tag{13}$$

$$(D_\mu\tilde{q})^{ij}=\partial_\mu\tilde{q}^{ij}-i((A_\mu)^i{}_k\tilde{q}^{kj}+\tilde{q}^{ik}(A_\mu^T)_k{}^j),$$
$$(A_\mu)^i{}_j=A_\mu^a(T_F^a)^i{}_j \tag{14}$$

$$D_\mu Q_i=\partial_\mu Q_i-i(A_\mu)_i{}^j\tilde{q}_j,$$
$$(A_\mu)_i{}^j=A_\mu^a(T_{\bar{F}}^a)_i{}^j=-A_\mu^a(T_F^{a,T})_i{}^j \tag{15}$$

$$(D_\mu c)^i{}_j=\partial_\mu c^i{}_j-i[A_\mu,c]^i{}_j, \qquad (A_\mu)^i{}_j=A_\mu^a(T_F^a)^i{}_j,$$
$$(c)^i{}_j=c^a(T_F^a)^i{}_j \tag{16}$$

and the 't Hooft coupling being $\lambda=g^2N_c$. We have chosen linear covariant gauge with gauge parameter ξ while $c=c^aT_F^a$ are ghost fields in the adjoint representation. This Lagrangian is equivalent to the canonically normalized Lagrangian in Eq. (A1) when appropriately rescaling the fields and carrying out the traces.

We can obtain the propagators by multiplying the canonically normalized propagators in Eq. (A8) by the completeness relations in Eqs. (9) and (10). We then obtain

$$\begin{aligned}
\langle(A_\mu(x))^i{}_j(A_\nu(y))^k{}_l\rangle&=\frac{1}{2}\Delta_{\mu\nu}(x-y)\frac{\lambda}{N_c}\left(\delta^i{}_l\delta^k{}_j-\frac{1}{N_c}\delta^i{}_j\delta^k{}_l\right)\\
\langle q_\alpha^i(x)\bar{q}_{\dot{\alpha},j}(y)\rangle&=S_{\alpha\dot{\alpha}}(x-y)\frac{\lambda}{N_c}\delta^i{}_j\\
\langle\tilde{q}_\alpha^{[ij]}(x)\bar{\tilde{q}}_{\dot{\alpha},[kl]}(y)\rangle&=\frac{1}{4}S_{\alpha\dot{\alpha}}(x-y)\frac{\lambda}{N_c}(\delta^i{}_l\delta^j{}_k-\delta^i{}_k\delta^j{}_l)\\
\langle Q_{\alpha,i,f}(x)\bar{Q}_{\dot{\alpha}}^{j,f'}(y)\rangle&=S_{\alpha\dot{\alpha}}(x-y)\frac{\lambda}{N_c}\delta_i{}^j\delta_f{}^{f'}\\
\langle(c(x))^i{}_j(\bar{c}(y))^k{}_l\rangle&=\frac{1}{2}\Delta(x-y)\frac{\lambda}{N_c}\left(\delta^i{}_l\delta^k{}_j-\frac{1}{N_c}\delta^i{}_j\delta^k{}_l\right)
\end{aligned} \tag{17}$$

for the propagators. Neglecting the Lorentz part of the propagators and only writing the color structure we present them as the following Feynman diagrams

$$\left\langle \left(A_\mu(x)\right)^i_{\ j} \left(A_\nu(y)\right)^k_{\ l} \right\rangle =$$

$$\left\langle q^i(x)\bar{q}_j(y) \right\rangle =$$

$$\left\langle \tilde{q}^{[ij]}(x)\bar{\tilde{q}}_{[kl]}(y) \right\rangle =$$

$$\left\langle Q_{i,f}(x)\overline{Q}^{j,f'}(y) \right\rangle =$$

$$\left\langle (c(x))^i_{\ j} (\bar{c}(y))^k_{\ l} \right\rangle =$$

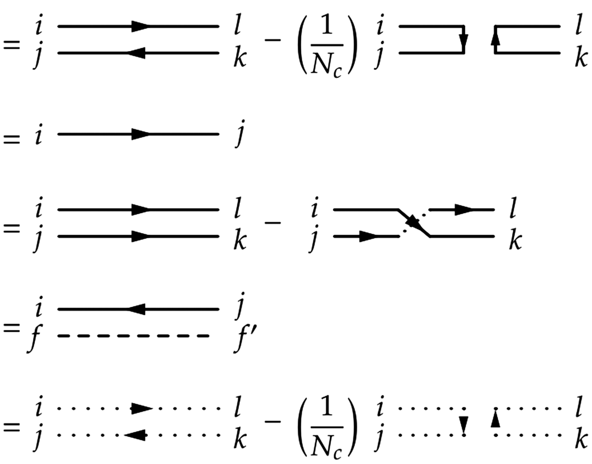

For simplicity we have not written an arrow on the flavor line for the Q propagator since it will always point in the same direction as the arrow on the associated color line.

III. SOME OBSERVATIONS

In this section we comment on a number of observations and properties of the chiral large N_c limit. First, counting of the degrees of freedom (neglecting spin) gives

$$\begin{aligned} A_\mu &: N_c^2 - 1 \xrightarrow{\text{large } N_c} N_c^2 \\ q_\alpha &: N_c \xrightarrow{\text{large } N_c} N_c \\ \tilde{q}_\alpha &: \frac{1}{2}N_c(N_c-1) \xrightarrow{\text{large } N_c} \frac{1}{2}N_c^2 \\ Q_{\alpha,f} &: N_c(N_c-3) \xrightarrow{\text{large } N_c} N_c^2 \end{aligned} \tag{18}$$

So the number of degrees of freedom of the q_α Weyl fermion only grows linearly as opposed to the degrees of freedom of all the other fields A_μ, $\tilde{q}_\alpha$, $Q_{\alpha,f}$ which grows quadratically. In other words the fundamental quark is suppressed.

Consider now the running of the 't Hooft coupling $\lambda = g^2 N_c$ which can be found from the running of the gauge coupling g. To one loop order the running is

$$\mu \frac{d\lambda}{d\mu} = -2\lambda \left[\tilde{b}_1 \frac{\lambda}{(4\pi)^2} + \ldots \right] \tag{19}$$

$$\begin{aligned} 3\tilde{b}_1 &= \underbrace{11}_{A_\mu} - \underbrace{\frac{1}{N_c}}_{q_\alpha} - \underbrace{\frac{N_c-2}{N_c}}_{\tilde{q}_\alpha} - \underbrace{\frac{N_c-3}{N_c}}_{Q_{\alpha,f}} \\ &\xrightarrow{\text{large } N_c} \underbrace{11}_{A_\mu} - \underbrace{1}_{\tilde{q}_\alpha} - \underbrace{1}_{Q_{\alpha,f}} \end{aligned} \tag{20}$$

So again we see that at the one loop level the fundamental quark q_α loops are suppressed by $1/N_c$ compared to the other A_μ, $\tilde{q}_\alpha$, $Q_{\alpha,f}$ loops. The theory is asymptotically free at any N_c.

At last consider the cancellation of the qubic gauge anomaly. The chiral large N_c extension is a chiral gauge theory and the qubic gauge anomaly is

$$\begin{aligned} SU(N_c)^3 &: \underbrace{1}_{q_\alpha} + \underbrace{(N_c-4)}_{\tilde{q}_\alpha} - \underbrace{(N_c-3)}_{Q_{\alpha,f}} = 0 \\ &\xrightarrow{\text{large } N_c} \underbrace{N_c}_{\tilde{q}_\alpha} - \underbrace{N_c}_{Q_{\alpha,f}} = 0 \end{aligned} \tag{21}$$

Again we see that the relevance of the fundamental quark q_α is suppressed relative to $\tilde{q}_\alpha$ and $Q_{\alpha,f}$ in canceling the gauge anomaly.

IV. LARGE N_c COUNTING

The $N_c \to \infty$ limit greatly simplifies the task of evaluating Feynman diagrams. Our most important task will be to keep track of powers of N_c.

In the large N_c limit we take the 't Hooft coupling λ to be fixed. As summarized in Eq. (17) propagators come with a factor of $\frac{1}{N_c}$. Interaction vertices come with a factor of N_c. Each color-, and flavor-contraction comes with a factor of $\sim N_c$

$$\delta^i_{\ i} = N_c, \qquad \delta^f_{\ f} = N_c - 3 \sim N_c \tag{22}$$

A. Gluons

We will first demonstrate how large N_c counting works for a pure Yang-Mills theory. Consider a simple vacuum bubble in double-line notation

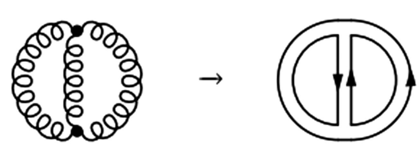

$\sim N_c^2$

In this work we take time to flow in the upward direction in all Feynman diagrams. To find the N_c scaling of this diagram, we only need to count propagators, vertices and color-loops. There are three propagators, two vertices, and three color-loops. In total, the diagram scales like $(\frac{1}{N_c})^3 \times N_c^2 \times N_c^3 \sim N_c^2$. As examples the following diagrams are also all $\sim N_c^2$

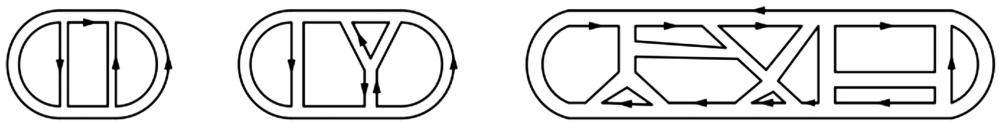

If we change the index-structure of the very first diagram, we can draw something subtly different

~ 1

This diagram has three propagators, two vertices and *one* loop, so it scales like $\sim(\frac{1}{N_c})^3 \times N_c^2 \times N_c \sim 1$. Relative to the other diagrams, this one is suppressed by $1/N_c^2$ which makes it irrelevant in the large N_c limit. The above examples hint at a hierarchy of Feynman diagrams in the large N_c limit—diagrams that can be drawn on a flat plane (planar diagrams) are dominant compared to the diagrams that require a third dimension to be drawn (nonplanar diagrams). One can now construct a $1/N_c$ expansion such that the sum over all N_c leading diagrams (the planar diagrams) samples a subsection of diagrams at all loop-orders. This is of course well known.

B. Fundamental quarks

Next, we can add q^i-quark lines to the vacuum bubbles. The counting rules are the same

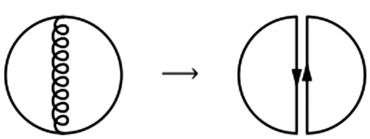

$$\sim \left(\frac{1}{N_c}\right)^3 \times N_c^2 \times N_c^2 = N_c$$

These kinds of diagrams scale like $\sim N_c$ because the quark line is a single color-line (as opposed to the gluon double-line). If we keep the diagram planar, but add some number of internal q^i-quark loops

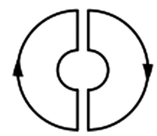

~ 1

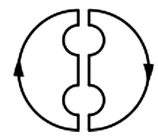

$\sim \frac{1}{N_c}$

we see that each internal quark loop gives a factor of $\frac{1}{N_c}$. So internal fundamental q^i-quark loops are suppressed. Yet another suppressed diagram with an internal q^i-quark loop is

$\sim \frac{1}{N_c}$

Of course, nonplanar diagrams are also still suppressed.

To sum up: If we want quarks in the diagram, the planar diagrams with a single quark loop on the boundary dominate. These diagrams scale as $\sim N_c$, which is subleading compared to the gluon vacuum bubbles $\sim N_c^2$.

C. Many antifundamental quarks

The antifundamental quarks $Q_{i,f}$ have a flavor-line in addition to their color-line. The consequence is that Q-quark loops are not suppressed, and internal Q-quark loops do not alter the N_c scaling

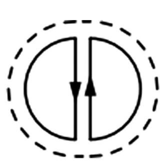

$\sim N_c^2$

$\sim N_c^2$

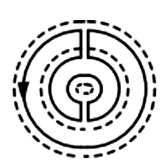

$\sim N_c^2$

In the third diagram we see that crossing flavor-lines with fermion- or gluon-lines is not suppressed. Second, planar diagrams still dominate over nonplanar ones

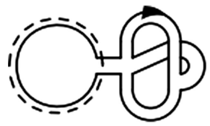

~ 1

Third, interrupted Q-quark loops, internal or not, are suppressed. The reason for this rule is that the interrupted quark loops reduce the number of color-loops. This becomes obvious when we use double-line notation

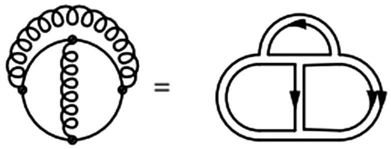

$\sim N_c^2$

The two index antisymmetric representation is the one used in the orientifold large N_c extension [35–39].

The vacuum bubble large N_c scaling of the various quark types is in agreement with the observations discussed in Sec. III. We know how to find the N_c scaling of any given diagram in the chiral large N_c extension and will now move on.

V. HADRON SPECTRUM

What are the minimal colorless hadrons in this theory? First, we have the order N_c-quark composites that only use one quark-type each

$$B = \epsilon_{i_1\ldots i_{N_c}} q^{i_1}\ldots q^{i_{N_c}}, \tag{23}$$

$$\tilde{B}_{N_c/2} = \epsilon_{i_1\ldots i_{N_c}} \tilde{q}^{[i_1 i_2]}\ldots\tilde{q}^{[i_{N_c-1} i_{N_c}]}, \qquad N_c \quad \text{even} \tag{24}$$

$$\tilde{B}_{\text{even}} = \epsilon_{i_1\ldots i_{N_c}}\epsilon_{j_1\ldots j_{N_c}} \tilde{q}^{[i_1 j_1]}\ldots\tilde{q}^{[i_{N_c} j_{N_c}]}, \quad N_c \quad \text{even} \tag{25}$$

$$\tilde{B}_{\text{odd}} = \epsilon_{i_1\ldots i_{N_c}}\epsilon_{j_1\ldots j_{N_c}} \tilde{q}^{[i_1 j_1]}\ldots\tilde{q}^{[i_{N_c} j_{N_c}]} = 0, \quad N_c \quad \text{odd} \tag{26}$$

$$\mathcal{B}_{f_1\ldots f_{N_c}} = \epsilon^{i_1\ldots i_{N_c}} Q_{i_1,f_1}\ldots Q_{i_{N_c},f_{N_c}} \tag{27}$$

We have suppressed the spinor-indices. It is clear that when $N_c = 3$ the composite $B = \epsilon_{ijk}q^i q^j q^k$ becomes the usual baryon Δ^{++} in one-flavor QCD. Note that the $\tilde{B}_{\text{odd}}$ composite vanishes

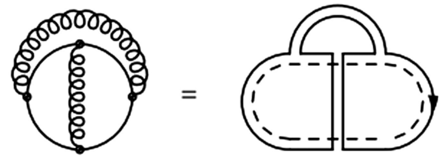

~ 1

D. Two-index antisymmetric quarks

The two-index antisymmetric quarks $\tilde{q}^{[ij]}$, similarly to the gluons, have two color-lines. In contrast to the Q-quark loops, interrupted $\tilde{q}$-quark loops have the same scaling as uninterrupted ones. In other words, *all* planar diagrams comprised of $\tilde{q}$'s and gluons, are $\sim N_c^2$—notice that this is the same scaling as in pure Yang-Mills

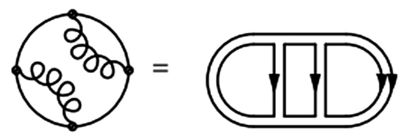

$\sim N_c^2$

$$\begin{aligned}\tilde{B}_{\text{odd}} &= \epsilon_{i_1\ldots i_{N_c}}\epsilon_{j_1\ldots j_{N_c}} \tilde{q}^{[i_1 j_1]}\ldots\tilde{q}^{[i_{N_c} j_{N_c}]} \\ &= (-1)^{N_c}\epsilon_{i_1\ldots i_{N_c}}\epsilon_{j_1\ldots j_{N_c}} \tilde{q}^{[j_1 i_1]}\ldots\tilde{q}^{[j_{N_c} i_{N_c}]} \\ &= -\epsilon_{j_1\ldots j_{N_c}}\epsilon_{i_1\ldots i_{N_c}} \tilde{q}^{[i_1 j_1]}\ldots\tilde{q}^{[i_{N_c} j_{N_c}]} = -\tilde{B}_{\text{odd}} = 0\end{aligned}$$

We can also build order N_c-quark composites by combining different quark-types. One combination is

$$M_{(1,N_c-2)} = \epsilon_{i_1\ldots i_{N_c}} \tilde{q}^{[i_1 i_2]} q^{i_3}\ldots q^{i_{N_c}} \tag{28}$$

This becomes the usual meson $M = \epsilon_{ijk}\tilde{q}^{[jk]}q^i$ when $N_c = 3$ in one-flavor QCD. For general N_c it is just one member of a whole family of composites. These consist of $\tilde{s}$ quarks and s fundamental quarks

$$M_{(\tilde{s},s)} = \epsilon_{i_1\ldots i_{N_c}} \tilde{q}^{[i_1 i_2]}\ldots\tilde{q}^{[i_{2\tilde{s}-1} i_{2\tilde{s}}]} q^{i_{2s+1}}\ldots q^{i_{N_c}}, \quad 2\tilde{s}+s = N_c \tag{29}$$

As we vary $\tilde{s}$ and s with $2\tilde{s}+s = N_c$ fixed, the $M_{(\tilde{s},s)}$ family of composites interpolates between the B and $\tilde{B}_{N_c/2}$ composites. When $\tilde{s} = 0$ and $s = N_c$ we have $M_{(0,N_c)} = B$ and when $\tilde{s} = N_c/2$ and $s = 0$ we have $M_{(N_c/2,0)} = \tilde{B}_{N_c/2}$. There are also the following two composites which consist of a fixed number of quarks not scaling with N_c

$$X_f = Q_{i,f}q^i \tag{30}$$

$$Y_{ff'} = \tilde{q}^{[ij]}Q_{i,f}Q_{j,f'} \tag{31}$$

The X_f's have the same color index contraction as the mesons in the 't Hooft limit, the difference being that they in addition have a single $SU(N_c-3)$ flavor index. The $Y_{ff'}$'s are also somewhat similar to the baryons in the Corrigan-Ramond extension [26] except for the two $SU(N_c-3)$ flavor-indices.

Finally, $\tilde{B}$ is the only composite exclusively made of two-index antisymmetric quarks that can be identified with an ordinary baryon. It consists of $N_c(N_c-1)/2$ quarks $\tilde{q}^{[ij]}$, and is nontrivial to write down for arbitrary N_c. In $SU(3)$, the two-index antisymmetric representation is the same as the antifundamental $\tilde{q}_i = \epsilon_{ijk}\tilde{q}^{[jk]}$, and the baryon is

$$\tilde{B}_{[SU(3)]} = \epsilon^{ijk}\tilde{q}_i\tilde{q}_j\tilde{q}_k = 2\epsilon_{i_1 j_1 j_2}\epsilon_{i_2 k_1 k_2}\tilde{q}^{[i_1 i_2]}\tilde{q}^{[j_1 j_2]}\tilde{q}^{[k_1 k_2]} \tag{32}$$

For $SU(4)$,

$$\begin{aligned}\tilde{B}_{[SU(4)]} = \Bigg(\sum_{\sigma\in S}&\mathrm{sign}(\sigma)\epsilon_{\alpha_{\sigma(4)}\beta_{\sigma(4)}\alpha_{\sigma(2)}\alpha_{\sigma(1)}}\\ &\times\epsilon_{\alpha_{\sigma(2)}\beta_{\sigma(5)}\beta_{\sigma(2)}\alpha_{\sigma(3)}}\epsilon_{\alpha_{\sigma(6)}\beta_{\sigma(6)}\beta_{\sigma(1)}\beta_{\sigma(3)}}\Bigg)\\ &\times\tilde{q}^{[\alpha_1\beta_1]}\tilde{q}^{[\alpha_2\beta_2]}\tilde{q}^{[\alpha_3\beta_3]}\tilde{q}^{[\alpha_4\beta_4]}\tilde{q}^{[\alpha_5\beta_5]}\tilde{q}^{[\gamma_3\delta_3]}\end{aligned} \tag{33}$$

The $\tilde{B}$ is the large N_c extension of this. It is constructed in such a way that it is an antisymmetric combination of all possible two-color labeled quarks, and it can be identified as the Skyrmion of the orientifold limit [31].

To sum up, for $N_c = 3$ the composites B, $\tilde{B}$ and $M_{(1,N_c-2)}$ are the standard baryons and meson, while the rest ($\tilde{B}_{N_c/2}$, $\tilde{B}_{\text{even}}$, $\mathcal{B}_{f_1\ldots f_{N_c}}$, $M_{(\tilde{s},s)}$, X_f, $Y_{ff'}$) all vanish. In terms of color-structure, every one of these composites also appear in the Corrigan-Ramond extension, except $\mathcal{B}_{f_1\ldots f_{N_c}}$, X_f and $Y_{ff'}$ which are unique in this chiral setting.

One can also include the conjugate quarks $\bar{q}_{\dot\alpha,i}$, $\bar{Q}^{i,f}_{\dot\alpha}$, $\bar{\tilde{q}}_{\dot\alpha,[ij]}$ and build conjugates of all the composites we have mentioned so far, as well as some additional ones, namely $q\bar{q}$ mesonlikes, arbitrarily large extensions of the tetraquark and flavor-analogs created by swapping any number of q's with Q's.

$$\begin{aligned}&q^i\bar{q}_i,\qquad \tilde{q}^{[ij]}\bar{\tilde{q}}_{[ij]},\qquad \tilde{q}^{[i_1 i_2]}\bar{\tilde{q}}_{[i_2 i_3]}\ldots\tilde{q}^{[i_{m-1}i_m]}\bar{\tilde{q}}_{[i_m i_1]}\\ &q^i\bar{\tilde{q}}_{[i_1 i_2]}\tilde{q}^{[i_2 i_3]}\ldots\tilde{q}^{[i_{m-1}i_m]}\bar{q}_{i_m},\qquad \tilde{q}^{[i_1 i_2]}\bar{\tilde{q}}_{[i_2 i_3]}\ldots\bar{\tilde{q}}_{[i_m i_{m+1}]}q^{i_m}q^{i_{m+1}},\\ &\quad+\text{flavor analogs}\,(q^i\to\bar{Q}^{i,f},\bar{q}_i\to Q_{i,f})\end{aligned}$$

We will consider these composites later in the text.

A. Hadron masses

In this section, we will use our large N_c tools to examine some of the properties and interactions of different composites in the theory. We will use diagrams and group-theoretical factors (quadratic Casimirs) to determine the masses of the composites. Afterward, we examine interactions between composites using large N_c diagram techniques.

1. Mass: Diagrams and combinatorics

First, we will use a diagrammatic approach. The goal is to examine gluon-corrections to the propagation of the hadrons with many quarks (which is every hadron except X_f and $Y_{ff'}$)

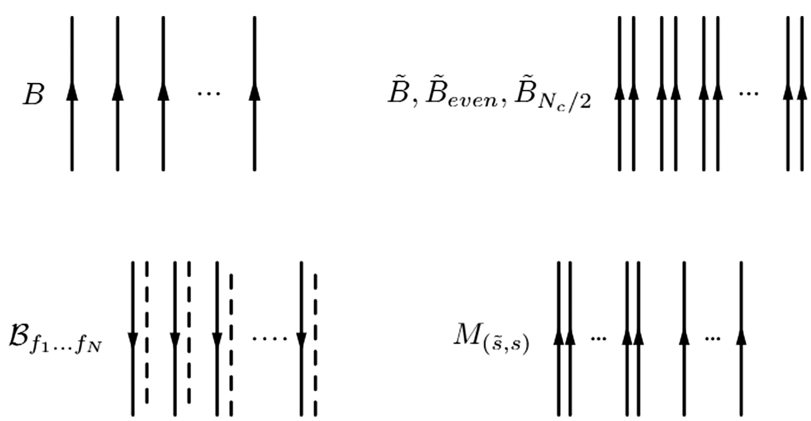

Gluon exchanges: The first-order correction to N_c-quark diagrams come from a one-gluon exchange between two of the confined quarks. The possible exchanges are

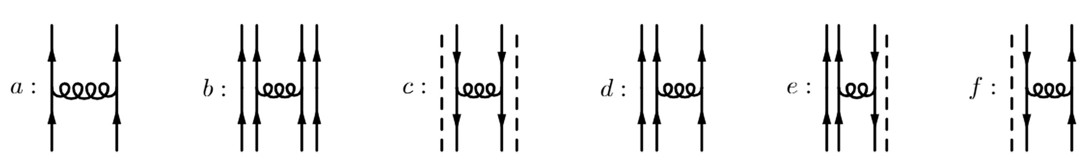

To specify what the color-flow of these diagrams look like, and then determine N_c-scaling, we burrow a procedure from [58] which is

(i) Select a suitable vacuum-bubble
(ii) Cut the quark lines twice to create the desired gluon-exchange
(iii) Find the N_c-scaling by examining how many loops are destroyed

We now comment on each of the one-gluon exchange diagrams above.

a: The first diagram is an exchange between two fundamental quarks. Using double-line notation

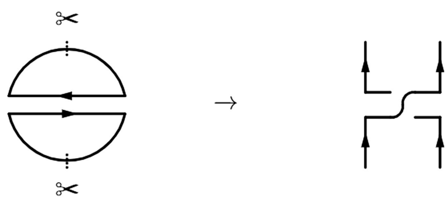

The diagram above show how to get gluon-exchange a by cutting a suitable vacuum bubble and twisting the gluon-propagator. Let us count N_c's: The vacuum bubble is $\sim N_c$, but cutting the quark-lines has the side-effect of destroying two color-loops $\sim 1/N_c^2$. In total this leaves us with $\sim \frac{1}{N_c}$ for the resulting diagram. Notice that our knowledge of the color-flow comes from the planar diagrams.

b: The second type of gluon exchange would be seen in the $\tilde{B}, \tilde{B}_{\mathrm{even}}, \tilde{B}_{\mathrm{simple}}$ baryons and the $M_{(\tilde{s},s)}$-family. A suitable diagram for analysis is a first-order correction to the $\tilde{q}^{[ij]}$ vacuum bubble

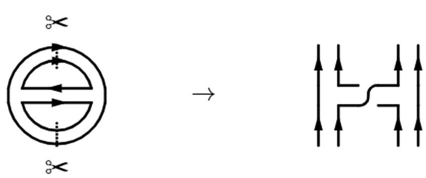

The vacuum bubble is $\sim N_c^2$ while cutting the quark-lines destroys three color-loops $\sim 1/N_c^3$. This leaves us with $\sim \frac{1}{N_c}$ in total.

c: The third type of gluon-exchange only shows up in the $\mathcal{B}_{f_1 \ldots f_{N_c}}$ baryons. Again, we should cut a suitable vacuum bubble diagram

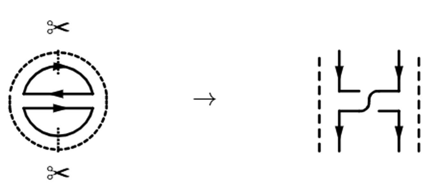

The vacuum bubble is $\sim N_c^2$ while cutting the quark-lines destroys one flavor-loop $\sim 1/N_c$ and two color-loops $\sim 1/N_c^2$. This leaves us with $\sim \frac{1}{N_c}$ in total.

d: The fourth type only shows up in the $M_{(\tilde{s},s)}$ composites. Cutting

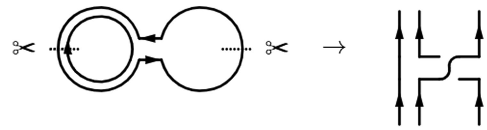

The vacuum bubble is $\sim N_c$ while cutting the quark-lines destroys both color-loops $\sim 1/N_c^2$. This leaves us with $\frac{1}{N_c}$.

e: The fifth type of gluon-exchange only happens in $Y_{f,f}$

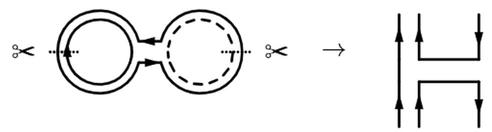

The vacuum bubble is $\sim N_c^2$ while cutting the quark-lines destroys one flavor-loop $\sim 1/N_c$ and two color-loops $\sim 1/N_c^2$. This leaves us with $\sim \frac{1}{N_c}$.

f: The sixth and final type of gluon exchange only happens in X_f

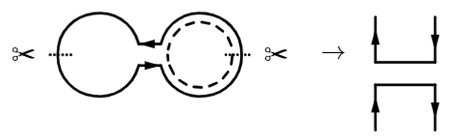

The vacuum bubble is $\sim N_c$ while cutting the quark-lines destroys one flavor-loop $\sim 1/N_c$ and one color-loop $\sim 1/N_c$. This leaves us with $\sim N_c \times \frac{1}{N_c} \times \frac{1}{N_c} = \frac{1}{N_c}$.

As we might have expected from an inspection of the Lagrangian, all of the one-gluon exchanges are of the same order in N_c. The next step in determining the mass of composites is to consider the combinatoric factors.

Combinatorics and mass: The combinatorics of the order N_c-quark composites are straightforward. They can each make $\sim N_c^2$ distinct quark pairs with each pair contributing with a $1/N_c$ gluon interaction. Thus, in total, the gluon interactions (and the masses of the composites) scale like $\sim \frac{1}{N_c} \times N_c^2 = N_c$.

The $\tilde{B}$ however, is a different story. When examining the combinatorics of the $\tilde{B}$, we have to consider a new subtlety [32]. A general one-gluon exchange changes the color-indices of a quark-pair from ij, kl to ik, jl

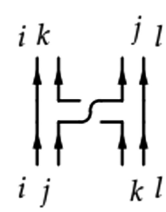

Because this baryon is an antisymmetric combination of all possible two-color labeled quarks, the ik, jl pair already exists in the $\tilde{B}$ composite. This violates Pauli's exclusion principle, and we must conclude that not all gluon exchanges are valid within the $\tilde{B}$ composite [32].[2] However, if the two quarks in the one-gluon exchange share *a single* color-index, the process does not change the color of the quark pair (up to a permutation)

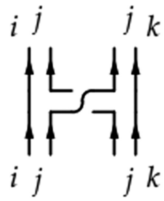

What does this mean for the combinatorics of a one-gluon exchange? When choosing the first quark, there are $\sim N_c^2$ to choose from, but for the second, there are only $\sim N_c$ quarks that share one color-index with the first. Combining these yields a total combinatoric factor of N_c^3. Gluon-interaction in the $\tilde{B}$ (and the mass) is thus $\sim \frac{1}{N_c} \times N_c^3 = N_c^2$.

For two-gluon exchanges, there are no restrictions on which quarks can participate. Therefore we have $\sim N_c^2$ choices for *both* the first *and* the second quark, giving a total combinatoric factor of N_c^4. Because two-gluon exchanges contribute as $\frac{1}{N_c^2}$,[3] the total contribution to the $\tilde{B}$ mass is again N_c^2

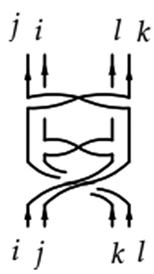

This argument can be extended to any and all classes of diagrams exclusively made of quarks in the two index antisymmetric representation [59]. The proof uses simplified equivalent diagrams by introducing "gluon-roundabouts."

The above analysis only includes two-body interactions. How does it extend to n-body interactions? We will again borrow a procedure from [58], and use the 't Hooft baryon B to argue that n-body interactions give the same result as two-body. If we for instance cut a planar vacuum bubble with three gluons into three pieces, we destroy three color-loops, ending up with a factor of N_c^{-2}. To balance this, when you choose three quarks from the baryon, it can be done N_c^3 ways. Again, the total contribution is N_c.

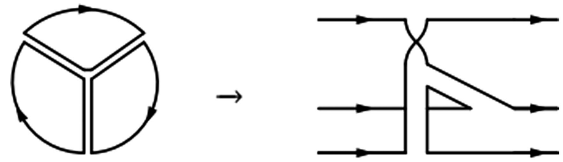

The generalization is that an n-body interaction scales like $N_c^{1-n} \times N_c^n = N_c$.

Lastly, d disconnected pieces contribute with N_c^d. When we uncover that $M_B \sim N_c$, it is easy to identify higher order contributions with the expansion of the propagator

$$e^{iM_B t} = 1 - iM_B t - \frac{M_B^2 t^2}{2} + \cdots \tag{34}$$

These points about n-body interactions and multiple disconnected pieces hold for the other hadrons as well. With this in mind, we will keep just discussing two-body interactions. One might worry that this kind of diagrammatic analysis is not rigorous enough, or maybe only holds for "heavy" quarks. To show that the results also are valid for light quarks, we will now perform an alternative set of calculations, and end up with the same results.

2. *Mass: Hamiltonian approach*

Another way of analyzing the masses of composites, is a "semirelativistic" approach described in [60] for light quarks.

Our simple baryon-Hamiltonian contains a relativistic kinetic term, and two potential terms. The one-gluon exchange potential V_{oge} contains contributions from all quark-pairs, and the confining potential V_c receives contributions from each quark:

$$\begin{aligned} H_{\text{baryon}} &= T + V_{oge} + V_c \\ &= \sum_{i=1}^{n_q} \left[\sqrt{\vec{p}_i^2} + a_q \sigma |\vec{x}_i - \vec{R}| \right] - \sum_{i<j=1}^{n_q} \frac{\lambda_0}{2} \frac{b_{q_1 q_2}}{|\vec{x}_i - \vec{x}_j|} \end{aligned} \tag{35}$$

where σ is the string tension between quarks (σ is expected to be independent of N_c at leading order [60]), and n_q is the number of quarks in the composite. The strength of both potentials depends on the *representation* of the quarks that are part of the baryon:

$$a_q = \frac{C_r}{C_F}, \qquad b_{q_1 q_2} = \frac{C_{r_1 \otimes r_2} - C_{r_1} - C_{r_2}}{N_c} \tag{36}$$

where C_r is the quadratic Casimir of the representation of a single quark in the composite, and $C_{r_1 \otimes r_2}$ is the quadratic Casimir of the representation of a pair of quarks undergoing a gluon-exchange. Clearly, the next step is finding the relevant quadratic Casimir operators. Using

[2] Note that this is not a problem for $\tilde{B}_{N_c/2}$, $\tilde{B}_{\text{even}}$ or $\tilde{M}_{(\bar{s},s)}$.

[3] If we insist on our procedure of cutting diagrams, the two-gluon exchange in the diagram can be obtained from a nonplanar diagram. This gives the $1/N_c^2$ factor.

TABLE II. The dimension, trace-normalization and quadratic Casimirs of all relevant representations. See part b) in the text for an explanation of why all these representations are relevant.

	d_r	T_r	C_r
$\ydiagram{1}$	N_c	$\frac{1}{2}$	$\frac{(N_c^2-1)}{2N_c}$
Adj	$(N_c+1)(N_c-1)$	$\frac{N_c-2}{2}$	N_c
$\ydiagram{1,1}$	$\frac{N_c(N_c-1)}{2}$	$\frac{N_c-2}{2}$	$\frac{(2N_c^2-2N_c-4)}{2N_c}$
$\ydiagram{2}$	$\frac{N_c(N_c+1)}{2}$	$\frac{N_c+2}{2}$	$\frac{(2N_c^2+2N_c-4)}{2N_c}$
$\ydiagram{2,1}$	$\frac{N_c(N_c-1)(N_c+1)}{3}$	$\frac{N_c^2-3}{2}$	$\frac{3(N_c^2-3)}{2N_c}$
$\ydiagram{1,1,1}$	$\frac{N_c(N_c-1)(N_c-2)}{6}$	$\frac{(N_c-3)(N_c-2)}{4}$	$\frac{3(N_c^2-2N_c-3)}{2N_c}$
$\ydiagram{2,2}$	$\frac{N_c^2(N_c+1)(N_c-1)}{12}$	$\frac{(N_c+2)N_c(N_c-2)}{6}$	$\frac{4(N_c+2)(N_c-2)}{2N_c}$
$\ydiagram{2,1,1}$	$\frac{(N_c+1)N_c(N_c-1)(N_c-2)}{8}$	$\frac{(N_c-2)(N_c^2-N_c-4)}{4}$	$\frac{4(N_c^2-N_c-4)}{2N_c}$
$\ydiagram{1,1,1,1}$	$\frac{N_c(N_c-1)(N_c-2)(N_c-3)}{24}$	$\frac{(N_c-2)(N_c-3)(N_c-4)}{12}$	$\frac{4(N_c+1)(N_c^2-N_c-4)}{2N_c}$
r_P	$N_c(N_c+1)(N_c-2)$	$\frac{(3N_c+1)(N_c-1)}{2N_c}$	$\frac{3N_c^2-2N_c-1}{2N_c}$

$$C_r = \frac{d_{\mathrm{Adj}}}{d_r} T_r = \frac{(N_c+1)(N_c-1)}{d_r} T_r \tag{37}$$

or equivalently, if one only knows the Dynkin indices $(a_1, a_2, \ldots, a_{N_c-1})$ of a representation,

$$C_r = \sum_{m=1}^{N_c-1} \Bigg[N_c(N_c-m) m a_m + m(N_c-m) a_m^2 + \sum_{n=0}^{m-1} 2n(N_c-m) a_n a_m \Bigg] \tag{38}$$

the relevant Casimir's are obtained and collected in Table II.

The confining potential: As summarized in Table III, the a_q-coefficients from (36) are all ~ 1. This means that all the composites have a contribution to their Hamiltonian proportional to the number of quarks $(\sim \sigma n_q)$, see Eq. (35).

The one-gluon exchange potential: Equation (35) instructs us to sum over all possible quark pairs that can undergo a one-gluon exchange. We will call the number of pairs P. See Table IV for a counting of pairs in each composite, and how much they each contribute to the one-gluon exchange potential. The next step is to insert the right b-coefficients into Table IV. But which ones should we use? There are six quarks-pairs, and each have multiple possible color-channels

$$\begin{aligned}
&\ydiagram{1} \otimes \ydiagram{1} = \ydiagram{2} \oplus \ydiagram{1,1}, \qquad \ydiagram{1} \otimes \overline{\ydiagram{1}} = \mathrm{Singlet} + \mathrm{Adj} \\
&\ydiagram{1,1} \otimes \ydiagram{1,1} = \ydiagram{2,2} \oplus \ydiagram{2,1,1} \oplus \ydiagram{1,1,1,1}, \qquad \ydiagram{1} \otimes \ydiagram{1,1} = \ydiagram{1,1,1} \oplus \ydiagram{2,1} \\
&\overline{\ydiagram{1}} \otimes \overline{\ydiagram{1}} = \overline{\ydiagram{1,1}} \oplus \overline{\ydiagram{2}},
\end{aligned} \tag{39}$$

The sixth tensor-product deserves more space and a dimensional check:

$$\ydiagram{1,1} \otimes \overline{\ydiagram{1}} = \ydiagram{1} \oplus \begin{array}{c} \ydiagram{2,2} \\ \vdots \\ \ydiagram{1} \end{array} \tag{40}$$

The last representation on the right-hand side (rhs) has $N_c - 1$ boxes in the first column, and two in the second. We will call this representation r_P because its shape resembles that of the letter P.

Having enumerated the different possible color-channels, we can now calculate their individual coefficients. As an example, see the following calculation

TABLE III. The color-channel-dependent coefficients of the confining potential V_c.

	C_r/C_F	Features in
$\ydiagram{1}$	1	$B, M_{(\tilde{s},s)}, X_f$
$\overline{\ydiagram{1}}$	1	$\mathcal{B}_{f_1 \ldots f_{N_c}}, X_f, Y_{ff'}$
$\ydiagram{1,1}$	$\frac{2(N_c-2)}{(N_c-1)}$	$\tilde{B}, \tilde{B}_{N_c/2}, \tilde{B}_{\mathrm{even}}, M_{(\tilde{s},s)}, Y_{ff'}$

TABLE IV. The different composites each have different number of quark-pairs, affecting the strength of the one-gluon potential V_{oge}. Notice that some composites have multiple different types of pairs. These are separated by a line-space.

	n_q	$2P$	Large N_c contribution to V_{oge}
B	N_c	$N_c \times (N_c - 1)$	$N_c^2 b_{qq}$
$\tilde{B}_{\text{even}}$	N_c	$N_c \times (N_c - 1)$	$N_c^2 b_{\tilde{q}\tilde{q}}$
$\tilde{B}_{N_c/2}$	$\frac{N_c}{2}$	$\frac{N_c}{2} \times (\frac{N_c}{2} - 1)$	$N_c^2 b_{\tilde{q}\tilde{q}}$
$\mathcal{B}_{f_1 \ldots f_{N_c}}$	N_c	$N_c \times (N_c - 1)$	$N_c^2 b_{QQ}$
$\tilde{\mathcal{B}}$	$\frac{N_c(N_c-1)}{2}$	$\frac{N_c(N_c-1)}{2} \times (\frac{N_c(N_c-1)}{2} - 1)$	$N_c^4 b_{\tilde{q}\tilde{q}}$
$M_{(1,N_c-2)}$	1	$1 \times (N_c - 1)/2$	$N_c b_{\tilde{q}Q}$
	$+(N_c - 1)$	$+(N_c - 1) \times (N_c - 2)$	$+N_c^2 b_{qq}$
$M_{(\tilde{s},s)}$	$\tilde{s}$	$\tilde{s}(\tilde{s} - 1)$	$\tilde{s}(\tilde{s} - 1) b_{\tilde{q}\tilde{q}}$
	$+s$	$+s(s - 1)$	$+s(s - 1) b_{qq}$
		$+\tilde{s}s$	$+\tilde{s}s b_{\tilde{q}Q}$
X_f	$1 + 1$	$1/2$	b_{qQ}
$Y_{f,f'}$	$1 + 2$	$3/2$	$2b_{Q\tilde{q}} + b_{\tilde{q}\tilde{q}}$

$$\begin{aligned} b_{\tilde{q}Q} &= \frac{1}{N_c} C_{r_P} - C_{\bar{F}} - C_{A2} \\ &= \frac{1}{2N_c^2} [3N_c^2 - 2N_c - 1 - (N_c^2 - 1) - (2N_c^2 - N_c - 2)] \\ &= \frac{1}{2N_c^2} [-N_c + 2] = +\frac{1}{N_c^2} - \frac{1}{2N_c} \end{aligned} \tag{41}$$

The results are gathered in Table V. When considering whether a color-channel is allowed, we should check if it gives rise to attractive or repulsive interactions between the quarks in the large N_c limit. This is also summarized in the table.

TABLE V. The color-coefficients for the one-gluon-exchange potential V_{oge}.

	Possible color channels	$b_{q_1 q_2}$	Attractive?
$\ydiagram{1} \otimes \ydiagram{1}$	$\ydiagram{2}$	$-\frac{1}{N_c^2} + \frac{1}{N_c}$	✗
	$\ydiagram{1,1}$	$-\frac{1}{N_c^2} - \frac{1}{N_c}$	✓
$\ydiagram{1} \otimes \overline{\ydiagram{1}}$	Adj.	$+\frac{1}{N_c^2}$	✗
	Singlet	$+\frac{1}{N_c^2} - 1$	✓
$\ydiagram{1} \otimes \ydiagram{1,1}$	$\ydiagram{2,1}$	$-\frac{2}{N_c^2} + \frac{1}{N_c}$	✗
	$\ydiagram{1,1,1}$	$-\frac{2}{N_c^2} - \frac{2}{N_c}$	✓
$\ydiagram{1,1} \otimes \ydiagram{1,1}$	$\ydiagram{2,2}$	$-\frac{4}{N_c^2} + \frac{2}{N_c}$	✗
	$\ydiagram{2,1,1}$	$-\frac{4}{N_c^2}$	✓
	$\ydiagram{1,1,1,1}$	$-\frac{4}{N_c^2} - \frac{4}{N_c}$	✓
$\ydiagram{1,1} \otimes \overline{\ydiagram{1}}$	r_P	$+\frac{1}{N_c^2} - \frac{1}{2N_c}$	✓
	$\ydiagram{1}$	$+\frac{2}{N_c^2} + \frac{1}{N_c} - 1$	✓
$\overline{\ydiagram{1}} \otimes \overline{\ydiagram{1}}$	$\overline{\ydiagram{2}}$	$-\frac{1}{N_c^2} + \frac{1}{N_c}$	✗
	$\overline{\ydiagram{1,1}}$	$-\frac{1}{N_c^2} - \frac{1}{N_c}$	✓

Notice that every tensor-product yields just one attractive representation except for $\ydiagram{1,1} \otimes \ydiagram{1,1}$ and $\ydiagram{1,1} \otimes \overline{\ydiagram{1}}$. Furthermore, the resulting color-channels (such as $\ydiagram{2,1,1}$ and $\ydiagram{1,1,1,1}$) have different large N_c behavior, so the distinction is important.

First, we will look at the choice between r_P and $\ydiagram{1}$. In this case, the b-coefficient for $\ydiagram{1}$ is ~ 1, and simply dominates over the coefficient for r_P which is $\sim 1/N_c$.

Next, the choice between $\ydiagram{2,1,1}$ and $\ydiagram{1,1,1,1}$. This is in fact what we treated in the combinatorics of the diagrammatic analysis. For $\tilde{B}_{N_c/2}, \tilde{B}_{\text{even}}$ and $M_{(\tilde{s},s)}$, the $\ydiagram{1,1,1,1}$ representation works just fine, and it also naturally dominates over $\ydiagram{2,1,1}$ (their b-coefficients are $\sim 1/N_c$ and $\sim 1/N_c^2$ respectively). However, $\tilde{\mathcal{B}}$ is constructed in such a way that a one-gluon exchange can only happen between quarks that share one color index. This is exactly what the $\ydiagram{2,1,1}$-representation does—two of the colors are symmetric as apparent from the Young tableu.

Finally, we can insert the attractive $b_{q_1 q_2}$ coefficients, and calculate V_{oge} for the different hadrons. The results are gathered in Table VI. To conclude on the one-gluon-potential: Once again, each hadron gets a contribution proportional to their number of quarks.

Bounds on hadron mass based on a_q and $b_{q_1 q_2}$: We have now seen how both the potentials of the Hamiltonian are of order n_q. Next, with a little help from [60], we can set an upper and lower bound for the masses of our composites

$$\begin{aligned} & n_q \inf_{|\psi\rangle} \langle\psi| \sqrt{\vec{p}^2} + \frac{n_q - 1}{2} \left[\frac{a_q}{n_q} r + \frac{b_{q_1 q_2}}{r} \right] |\psi\rangle \\ & \leq M_{\text{composite}} \leq \sqrt{4a_q (Q n_q - b_{q_1 q_2} P^{3/2})} \end{aligned} \tag{42}$$

TABLE VI. Final contributions to the one-gluon-potential V_{oge} after calculating number of pairs, and then weighing each pair with their respective quadratic Casimir.

	n_q	Large N_c contribution to V_{oge}
B	N_c	N_c
$\tilde{B}_{N_c/2}$	$N_c/2$	N_c
$\tilde{B}_{\text{even}}$	$\frac{N_c}{2}$	N_c
$\mathcal{B}_{f_1 \ldots f_{N_c}}$	N_c	N_c
$\tilde{B}$	$\frac{N_c(N_c-1)}{2}$	N_c^2
M_1	$1+(N_c-2)$	N_c
$M_{(\tilde{s},s)}$	$\tilde{s}+s$	$\frac{\tilde{s}s+\tilde{s}(\tilde{s}-1)+s(s-1)}{N} \sim N_c$
X_f	$1+1$	1
$Y_{f,f'}$	$1+2$	1

where $Q \sim n_q$ is the band number of the considered state in a harmonic oscillator picture. Inserting into Eq. (42) and taking the large N_c limit, we again arrive at the masses with the same N_c scaling as $\sim n_q$.

Before moving on, we should note a detail about the masses of $\tilde{B}_{N_c/2}$ and $\tilde{B}_{\text{even}}$. Because they are symmetric in their gauge-functions under exchange of two quarks, they receive a contribution from Fermi zero temperature pressure (which maximally scales like $\sim N_c^{4/3}$) [31].

B. Hadron interactions

1. Interactions: Scattering diagrams

Following a diagrammatic analysis similar to Witten [10], we can get a heuristic idea about how scattering between the different hadrons $(B, \tilde{B}_{N_c/2}, \tilde{B}_{\text{even}}, \tilde{B}, \mathcal{B}_{f_1\ldots f_{N_c}}, M_{(\tilde{s},s)}, X_f, Y_{ff'})$ scale with N_c.[4]

The idea is to examine all possible exchanges between the hadrons, using the gluon exchanges from Sec. VA 1. To evaluate the final effect of these diagrams, we have to develop a procedure to determine the associated combinatoric factors. To establish this procedure, we should study some examples:

Exchanges between B and X_f: How might these interact? They could exchange a quark, gluon or both. Let us draw all possible diagrams up to one-gluon exchange

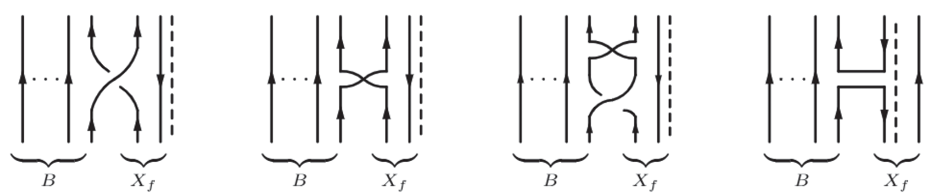

When evaluating these diagrams, we need to take into account nontrivial combinatoric factors. To highlight this, we look closer at the quark-quark exchange channel with one gluon (the second and third diagrams).

First, assign a color i to the in-going quark from composite with lowest n_q, in this case X_f. This gives a combinatoric factor of 1 (there is *one* fundamental quark in X_f to choose from). Follow the color-flow, and carry the color to where it ends

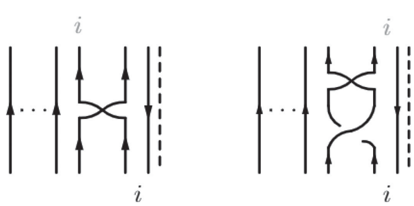

Next, the color of all in-going quarks should match their outgoing color for the hadron to be gauge invariant. We should assign the i to the outgoing quark from X_f, and follow the color-flow again (this time backward)

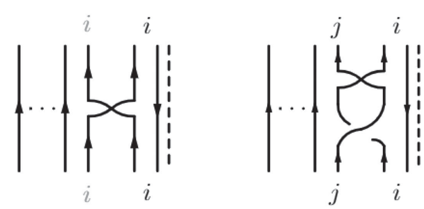

At this point the diagrams differ. The colors of the first diagram are fully determined giving a combinatoric factor of 1 (there is only *one* quark in B with the color i), while there is an undetermined color index j in the second diagram giving a combinatoric factor N_c (there are N_c quarks in B with an arbitrary color). Thus, the diagrams (with combinatoric factors) contribute $1/N_c$ and 1 respectively, so $\mathcal{M}(B, X_f)_{\text{scattering}} \sim 1$. This is strong enough to affect the X_f's, but not the 't Hooft baryons.

If we had instead examined the q-Q channel (the fourth diagram above), we would have found that diagram to contribute $\sim 1/N_c$. It is a trend that *cross-quarktype*

[4]It should be noted that this analysis is at fixed velocity and not fixed momentum because many of the hadrons have N_c-scaling masses.

channels are suppressed—although sometimes they are still the most dominant channels.

$\tilde{q}$ combinatoric factors: Because $\tilde{B}$ has $N_c(N_c-1)$ quarks, it can give a larger combinatoric factor than, e.g., $B_{N_c/2}$ with $N_c/2$ quarks. Lets see an example of this by examining their respective interaction with $\mathcal{B}_{f_1\ldots f_{N_c}}$:

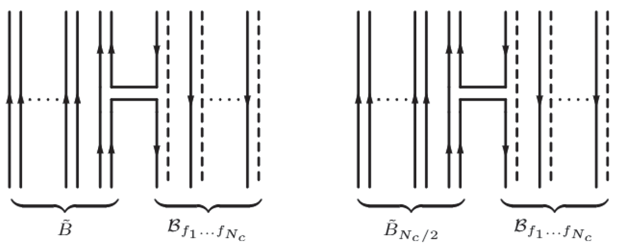

In both diagrams, the interacting quark has one determined color i, and one free color. For the interaction with $\tilde{B}$, this means a combinatoric factor of N_c (there are N_c quarks in $\tilde{B}$ with color i). For $\tilde{B}_{N_c/2}$, the combinatoric factor is 1 (there is just *one* quark in $\tilde{B}_{N_c/2}$ with color i). We conclude that $\mathcal{M}(\tilde{B},\mathcal{B}_{f_1\ldots f_{N_c}})_{\text{scattering}}\sim N_c$ (strong enough to affect $\mathcal{B}_{f_1\ldots f_{N_c}}$ but not $\tilde{B}$), while $\mathcal{M}(\tilde{B}_{N_c/2},\mathcal{B}_{f_1\ldots f_{N_c}})_{\text{scattering}}\sim 1$ (not strong enough to affect either of the interacting hadrons).

Next, compare the scattering amplitudes for pairs (B,X_f) and $(\tilde{B}_{N_c/2},Y_{ff'})$. Naively, one might think that the amplitudes should be the same—the $B,\tilde{B}_{N_c/2}$'s are somewhat similar in structure, the X, Y's are similar, and both pairs can exchange a quark of the same type

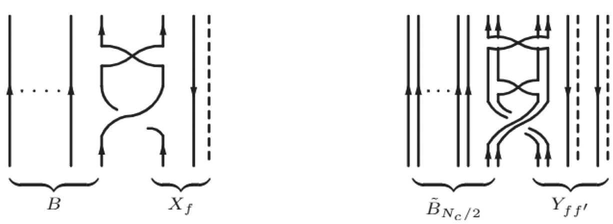

We have already seen that $\mathcal{M}(B,X_f)_{\text{scattering}}\sim 1$ for the first diagram. In the second diagram, the two gluons give $1/N_c^2$, there is 1 quark to choose from in Y, and $N_c/2$ quarks to choose from in $\tilde{B}_{N_c/2}$. In total, we get $\mathcal{M}(\tilde{B}_{N_c/2},Y_{ff'})_{\text{scattering}}\sim 1/N_c$. The $\tilde{B}_{N_c/2}$'s do not affect the $Y_{ff'}$'s even though they have quark content in common.

The two amplitudes differ because of the two index antisymmetric quarks $\tilde{q}^{[ij]}$. A quark $\tilde{q}^{[ij]}$ exchange requires *two* gluon exchanges for the colors to be independent of each other. This allows for large combinatoric factors when $\tilde{B}$ is involved, but also serves to suppress quark exchanges in $\tilde{B}_{N_c/2},\tilde{B}_{\text{even}},M_{(\tilde{s},s)}$.

$M_{(\tilde{s},s)}$ counting: Because they have a variable number of quarks q^i and $\tilde{q}^{[ij]}$, the $M_{(\tilde{s},s)}$ exchanges require a little more of a delicate counting. Let us examine the scattering amplitudes for the pair $(M_{(\tilde{s},s)},B)$

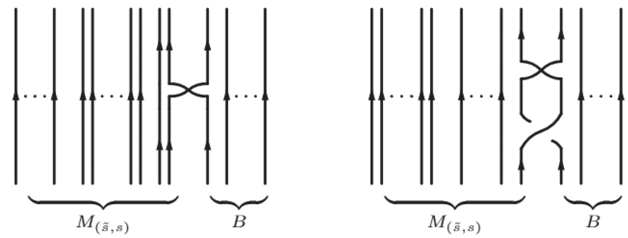

The first diagram, with combinatoric factors, contributes $\sim\frac{1}{N_c}\times\tilde{s}\times 2\sim\frac{\tilde{s}}{N_c}$ (there are $\tilde{s}$ quarks to choose from, and one quark in B with matching colors). The second diagram, with combinatoric factors, contributes $\sim\frac{1}{N_c}\times s\times N_c=s$. The second diagram dominates, and we get $\mathcal{M}(M_{(\tilde{s},s)},B)_{\text{scattering}}\sim s$.

General procedure: For two composites v, w with $n_q(v)\le n_q(w)$, the general procedure for determining the combinatoric factor is

(i) Assign colors to the ingoing quark q_1 from w. Follow the color-flow and assign colors to wherever they end up.

(ii) Assign the same colors to the outgoing quark q_1 from w, and follow the color-flow backward to again ensure that the colors are consistent.

(iii) Determine the two combinatoric factors by asking,
a: How many quarks could I have chosen for step 1?
b: How many quarks in v have colors that are consistent with those determined in step 1 and 2.

Now we have the tools to examine interactions between any hadron. Exhausting every possible one-gluon interaction (or two-gluon when two index antisymmetric quarks $\tilde{q}^{[ij]}$ are exchanged), we arrive at Table VII: The scattering amplitudes should be compared to the masses of the involved hadrons. This is done in Table VIII: We can make a few interesting observations from Table VIII.

TABLE VII. Scattering amplitudes between the different hadrons. Notice that if the two hadrons have no quark content in common, the interaction can be suppressed.

	$\tilde{B}$	$\tilde{B}_{N_c/2}$	$\tilde{B}_{\text{even}}$	$M_{(\tilde{s},s)}$	B	$\mathcal{B}_{f_1\ldots f_{N_c}}$	X_f	$Y_{f,f'}$
$\tilde{B}$	N_c^2	N_c	N_c	N_c	N_c	N_c	1	1
$\tilde{B}_{N_c/2}$	N_c	1	1	1	1	1	$1/N_c$	$1/N_c$
$\tilde{B}_{\text{even}}$	N_c	1	1	1	1	1	$1/N_c$	$1/N_c$
$M_{(\tilde{s},s)}$	N_c	1	1	s	s	1	s/N_c	$1/N_c$
B	N_c	1	1	s	N_c	1	1	$1/N_c$
$\mathcal{B}_{f_1\ldots f_{N_c}}$	N_c	1	1	1	1	N_c	1	1
X_f	1	$1/N_c$	$1/N_c$	s/N_c	1	1	$1/N_c$	$1/N_c$
$Y_{f,f'}$	1	$1/N_c$	$1/N_c$	$1/N_c$	$1/N_c$	1	$1/N_c$	$1/N_c$

TABLE VIII. Qualitative analysis of scattering amplitudes. If the amplitude is strong enough to affect the motion of one of the involved hadrons, we write a checkmark in the direction of that hadron.

	$\tilde{B}$	$\tilde{B}_{N_c/2}$	$\tilde{B}_{even}$	$M_{(\tilde{s},s)}$	B	$\mathcal{B}_{f_1\ldots f_{N_c}}$	X_f	$Y_{f,f'}$
$\tilde{B}$	✓ / ✓	✓ / ×	✓ / ×	✓ / ×	✓ / ×	✓ / ×	✓ / ×	✓ / ×
$\tilde{B}_{N_c/2}$	× / ✓	× / ×	× / ×	× / ×	× / ×	× / ×	× / ×	× / ×
$\tilde{B}_{even}$	× / ✓	× / ×	× / ×	× / ×	× / ×	× / ×	× / ×	× / ×
$M_{(\tilde{s},s)}$	× / ✓	× / ×	× / ×	if $s\sim N_c$	if $s\sim N_c$	× / ×	if $s\sim N_c$	× / ×
B	× / ✓	× / ×	× / ×	if $s\sim N_c$	✓ / ✓	× / ×	✓ / ×	× / ×
$\mathcal{B}_{f_1\ldots f_{N_c}}$	× / ✓	× / ×	× / ×	× / ×	× / ×	✓ / ✓	✓ / ×	✓ / ×
X_f	× / ✓	× / ×	× / ×	if $s\sim N_c$	× / ✓	× / ✓	× / ×	× / ×
$Y_{f,f'}$	× / ✓	× / ×	× / ×	× / ×	× / ×	× / ✓	× / ×	× / ×

(i) The $\tilde{B}$ only scatters with itself, but affects the motion of everything else around. The $\tilde{B}_{N_c/2}$ and $\tilde{B}_{\rm even}$ on the other hand affect nothing, and are only scattered by $\tilde{B}$.

(ii) The usual meson $M_{(1,N_c-2)}$ and the 't Hooft baryon B scatter with each other. This might be seen as an attractive feature of the large N_c limit because it resembles what happens in the $N_c = 3$ theory.

(iii) The X_f and $Y_{ff'}$'s are scattered by $\mathcal{B}_{f_1\ldots f_{N_c}}$ and $\tilde{B}$. The B and $M_{(\tilde{s},s)}$ can also push around the X_f's because they all feature fundamental quarks.

The general pattern is that scattering amplitudes between hadrons follow a number-of-quarks- and quark-type hierarchy: The hadrons with $n_q \sim N_c^2$ interact with all other hadrons, and are only scattered only by themselves. Hadrons with $n_q \sim N_c$ scatter with each other if they have a sufficient amount of quark content in common. Hadrons with $n_q \sim 1$ are scattered by higher $n_q \sim N_c$-hadrons if they have a sufficient number of quarks of the same type as the $n_q \sim 1$-hadron. For fundamental and antifundamental quarks, this "sufficient" number of quarks is $\sim N_c$, and for two index quarks it is $\sim N_c^2$.

2. Interactions: Correlation functions

The X_f and $Y_{ff'}$ composites have $n_q \sim 1$, so we can use correlation function analysis to examine them. Before calculating any correlation functions, note that insertions of X_f and $Y_{ff'}$ on quark lines are quite limited. They must appear pairwise. The possible insertions are

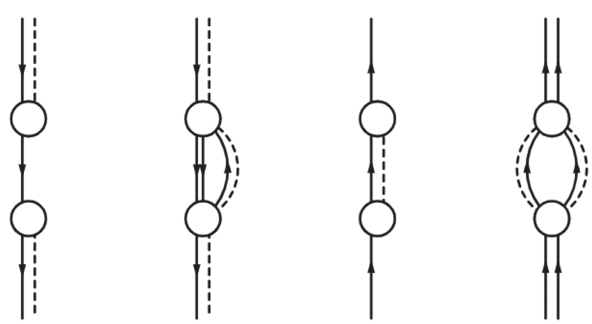

Notice that the two insertions of $Y_{ff'}$ on an antifundamental line yield an extra color-loop, but also breaks up a potential flavor-loop (remember the arrows on the flavor-lines follow those of the quark color-lines).

$\mathbf{Y_{f,f'}}$: It is only possible to draw *even* n_Y-point functions of $Y_{f,f'}$. The leading order contributions to the generating functional from $Y_{f,f'}$ are of order $N_c^{1+n_Y/2}$, and they look something like this:

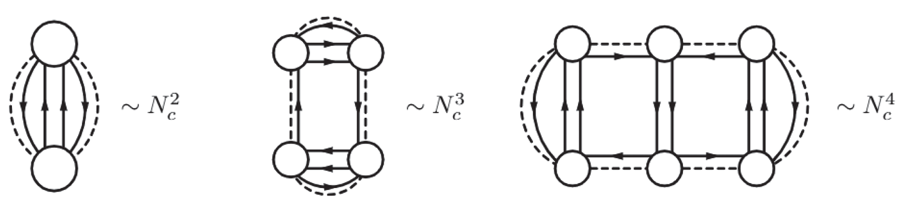

Note that instead of forming loops, the flavors are simply propagating between hadrons (remember that the flavor-lines also carry arrows with the same direction as their associated color line). Adding sources, we learn that we should include a factor of N_c in the definition of $\hat{Y}_{f,f'}$ if we want the two-point function to be of order 1. Thus, a general n_Y point function goes like:

$$\langle Y(x)Y(y)\rangle = \frac{1}{N_c^2}\frac{\delta}{\delta J(x)}\frac{\delta}{\delta J(y)}\log(Z[J]_{J\equiv 0}) \sim 1 \qquad (43)$$

$$\langle\underbrace{Y\cdots Y}_{n_Y}\rangle \sim \frac{1}{N_c^{n_Y}} \times N_c^{1+n_Y/2} = N_c^{1-n_Y/2} \qquad (44)$$

As a result of this behavior, the Y's by themselves are stable, free particles ($\langle YYYY\rangle \sim N_c^{-1}$). Furthermore, because the operator is single-trace, and the theory is asymptotically free, we expect the $N_c \to \infty$ world to feature an infinite tower of single-particles states [10].

$\mathbf{X_f}$: The fact that the X_f's consists of two different quark types, means that they also have to appear in pairs. The leading order contributions to $\log(Z[J])$ comes from processes like

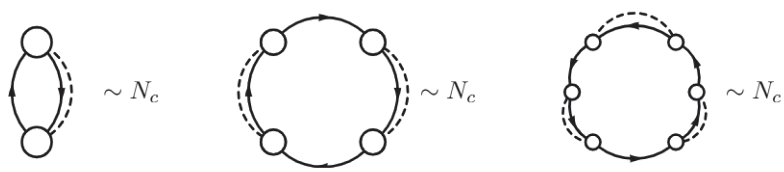

Like the standard meson operator, the diagrams contributing to n_X-point functions are always $\sim N_c$. Consequently, they have to be normalized by a factor $\sqrt{N_c}$, and a general n_X-point function is

$$\langle\underbrace{X\cdots X}_{n_x}\rangle \sim \frac{1}{N_c^{n_X/2}} \times N_c = N_c^{1-n_X/2} \qquad (45)$$

This is exactly similar to the Y composite, and the conclusions that one can draw from it are the same.

Mixing X's and Y's: It is easy to create diagrams with both X, and Y operators. The general structure can be constructed by starting with the skeleton of a $\langle YY\rangle$ diagram. Then insert n_X X's two at a time on an arbitrary Q line, and add n_Y $Y's$ two at a time, directly connecting to the previous YY pair. Because the X's do not change the N_c-counting, the resulting diagram contributes $N_c^{1+n_Y/2}$

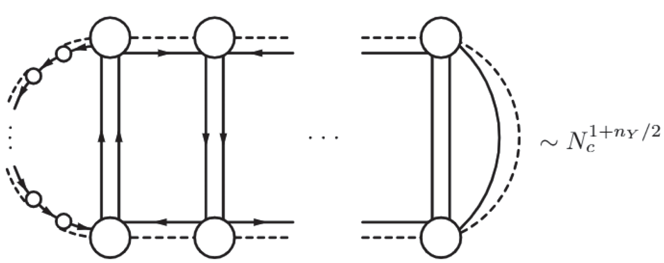

Now, an arbitrary n-point function is

$$\langle\underbrace{X\cdots X}_{n_x}\underbrace{Y\cdots Y}_{n_Y}\rangle \sim \frac{1}{N_c^{n_X/2+n_Y}} \times N_c^{1+n_Y/2} = N_c^{1-n_X/2-n_Y/2} \qquad (46)$$

The mixed correlation function of highest order in N_c is $\langle XXYY\rangle \sim N_c^{-1}$, so interactions are suppressed.

Do the X and Y mix with the glueballs? The glueballs can be inserted arbitrarily on available gluon-lines without changing the value of a diagram. And because of planarity, there are available gluon-lines everywhere. All in all then, each glueball adds a factor of $N_c^{-n_G}$ in the correlation functions, because of their normalization

$$\langle\underbrace{X\cdots X}_{n_x}\underbrace{Y\cdots Y}_{n_Y}\underbrace{G\cdots G}_{n_G}\rangle \sim \frac{1}{N_c^{n_X/2+n_Y+n_G}} \times N_c^{1+n_Y/2} = N_c^{1-n_X/2-n_Y/2-n_G} \qquad (47)$$

We conclude that interactions with glueballs are also suppressed.

3. Interactions: Diagrams for additional processes

The gauge structure of our composites also allow for nontrivial processes although many of them are suppressed. They all conserve the two $U(1)$ symmetries from Table I as they should.

X_f and $Y_{ff'}$ insertions: The X_f and $Y_{ff'}$'s can be inserted on the baryon lines. They have to be inserted two at a time, and they each bring normalization factors $\sqrt{N_c}$, and N_c respectively for X_f and $Y_{ff'}$. The color-flow of the baryon lines thus allows for the creation of an $X_f\bar{X}^f$ pair (or $Y_{ff'}\bar{Y}^{ff'}$ pair), or scattering between a baryon and X_f (or $Y_{ff'}$). Some examples are

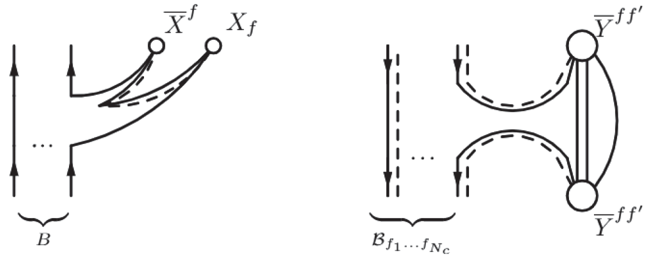

The amplitudes for a baryon $(B, \mathcal{B}_{f_1 \dots f_{N_c}})$ to scatter with X_f or create an $X_f \bar{X}^f$ pair, are the same

$$\mathcal{M} \sim \underbrace{N_c^{-1}}_{\text{Normalization factors}} \times \underbrace{N_c}_{\text{Combinatorics}} = 1 \tag{48}$$

Creating a pair of particles would of course also require the baryon to transition to a lower energy-state. The amplitudes for a baryon $(\mathcal{B}_{f_1 \dots f_{N_c}}, \tilde{B}, \tilde{B}_{\text{even}}, \tilde{B}_{N_c/2})$ to scatter with $Y_{ff'}$ or create a $Y_{ff'} \bar{Y}^{ff'}$ pair are also the same, but they depend on which baryon one chooses.

For $\tilde{B}_{\text{even}}, \tilde{B}_{N_c/2}$, the amplitude is

$$\mathcal{M} \sim \underbrace{N_c^{-2}}_{\text{Normalization factors}} \times \underbrace{N_c}_{\text{Combinatorics}} = \frac{1}{N_c} \tag{49}$$

For $\mathcal{B}_{f_1 \dots f_{N_c}}$, the amplitude is

$$\mathcal{M} \sim \underbrace{N_c^{-2}}_{\text{Normalization factors}} \times \underbrace{N_c}_{\text{Color loop}} \times \underbrace{N_c}_{\text{Combinatorics}} = 1 \tag{50}$$

For $\tilde{B}$, the amplitude is

$$\mathcal{M} \sim \underbrace{N_c^{-2}}_{\text{Normalization factors}} \times \underbrace{N_c^2}_{\text{Combinatorics}} = 1 \tag{51}$$

These results are compatible with Table VIII.

Baryonium states: Next, as an analog of baryonium states in the 't Hooft limit [10,61], a single $\mathcal{B}_{f_1 \dots f_{N_c}}$ may combine with B or $\tilde{B}_{N_c/2}$ to form a "baryonium" bound-state $B\mathcal{B}_{f_1 \dots f_{N_c}}$ or $\tilde{B}_{N_c/2}\mathcal{B}_{f_1 \dots f_{N_c}}$. First consider the $B\mathcal{B}_{f_1 \dots f_{N_c}}$ state. With the inclusion of combinatoric factors, interactions between the fundamental and antifundamental quarks inside this state are $\sim N_c$

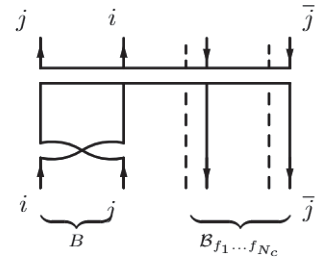

It is possible for $B\mathcal{B}_{f_1 \dots f_{N_c}}$ to decay via successive emissions of X_f's. See Feynman diagram below. After one such emission, we will call the resulting state $B\mathcal{B}_{f_1 \dots f_{N_c - 1}}(1)$. In this state, the remaining $(N_c - 1)$ quarks $\epsilon_{i_1 \dots i_{N_c}} q^{i_1} \dots q^{i_{N_c-1}}$ form an antifundamental representation, and the remaining $(N_c - 1)$ flavored quarks $\epsilon^{i_1 \dots i_{N_c}} Q_{i_1, f_1} \dots Q_{i_{N_c-1}, f_{N_c-1}}$ form a fundamental representation. In this sense, such a state behaves like a $q^i \bar{q}_i$ operator—it is capable of producing color-loops, and should be normalized accordingly.

From this state, another meson may be emitted, and then another, and so on. A general baryonium state obtained by C emissions is then $B\mathcal{B}_{f_1 \dots f_{N_c - C}}(C)$. We can write such a decay as

$$B\mathcal{B}_{f_1 \dots f_{N_c - C}}(C) \to B\mathcal{B}_{f_1 \dots f_{N_c - (C+1)}}(C+1) + X_f \tag{52}$$

The following diagram represents the first process in which $B\mathcal{B}_{f_1 \dots f_{N_c}}$ emits the first meson X_f

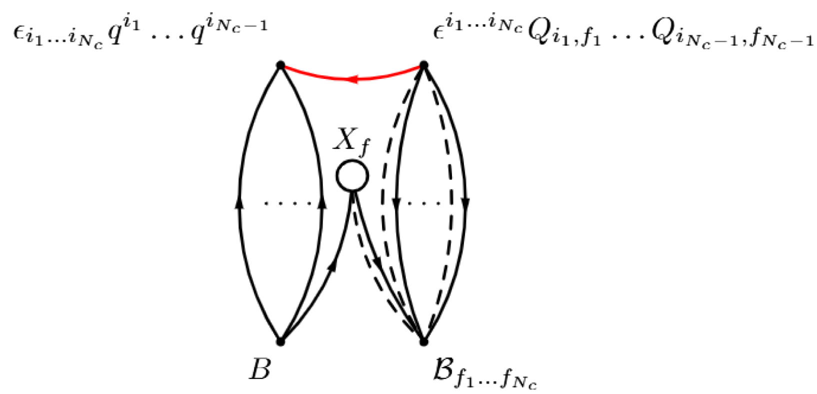

Here, the colored line is not a quark-line. Rather, it represents the fact the antifundamental $\epsilon_{i_1 \ldots i_{N_c}} q^{i_1} \ldots q^{i_{N_c-1}}$ and fundamental $\epsilon^{i_1 \ldots i_{N_c}} Q_{i_1, f_1} \ldots Q_{i_{N_c-1}, f_{N_c-1}}$ states combine to form a gauge-singlet. The amplitude for an arbitrary X_f emission is

$$\mathcal{M}_{B\mathcal{B}(C)\to B\mathcal{B}(C+1)} \sim \underbrace{\frac{1}{N_c^{C/2}} \times \frac{1}{N_c^{(C+1)/2}} \times \frac{1}{N_c^{1/2}}}_{B\mathcal{B}, X_f \text{Normalization factors}} \times \underbrace{(N_c - C)}_{\text{Combinatoric factor}} \times \underbrace{N_c^C}_{\text{Color loops}} = \frac{N_c - C}{N_c} \tag{53}$$

The amplitude starts at ~ 1 when the bound state consists of $2N_c$ quarks, and ends at $\sim \frac{1}{N_c}$ when there are two quarks left.

In the other baryonium state $\tilde{B}_{N_c/2} \mathcal{B}_{f_1 \ldots f_{N_c}}$ there again exists interactions between the Q and $\tilde{q}$ which are $\sim N_c$. This baryonium state decays via successive emissions of $Y_{ff'}$'s. The following diagram represents the first emission

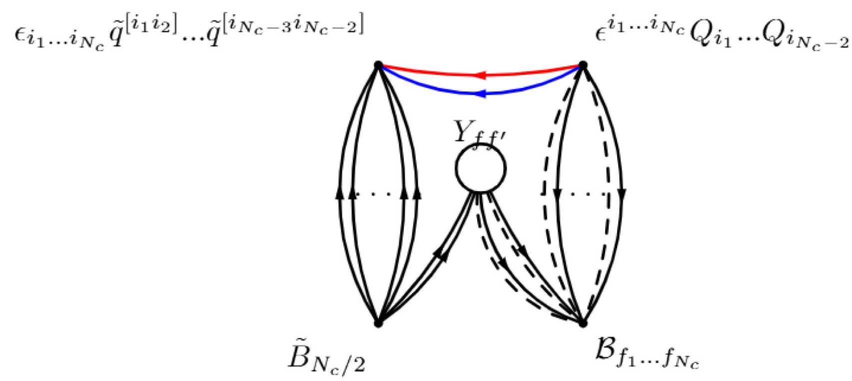

The amplitude for this process is

$$\mathcal{M}_{\tilde{B}_{N_c/2}\mathcal{B}(C)\to \tilde{B}_{N_c/2}\mathcal{B}(C+1)} \sim \underbrace{\frac{1}{N_c^C} \times \frac{1}{N_c^{C+1}} \times \frac{1}{N_c}}_{\tilde{B}\mathcal{B}, Y_{ff'} \text{Normalization factors}} \times \underbrace{\frac{N_c}{2} - C}_{\text{Combinatoric factor}} \times \underbrace{N_c^{2C}}_{\text{Color loops}} = \frac{N_c/2 - C}{N_c^2} \tag{54}$$

The amplitude starts at $\sim \frac{1}{N_c}$ when there are $\frac{3}{2} N_c$ bound quarks and ends at $\sim \frac{1}{N_c^2}$ when there are three quarks left. The $\tilde{B}_{N_c/2-C} \mathcal{B}_{f_1 \ldots f_{N_c-C}}(C)$ states are thus narrower than the $B\mathcal{B}_{f_1 \ldots f_{N_c-C}}(C)$ states by a factor of N_c.

A nontrivial scattering process: We now consider the following nontrivial scattering process

$$M_{(\tilde{s},s)} + Y_{ff'} \to 2X_f + M_{(\tilde{s}+1, s-2)} \tag{55}$$

Diagrammatically it is

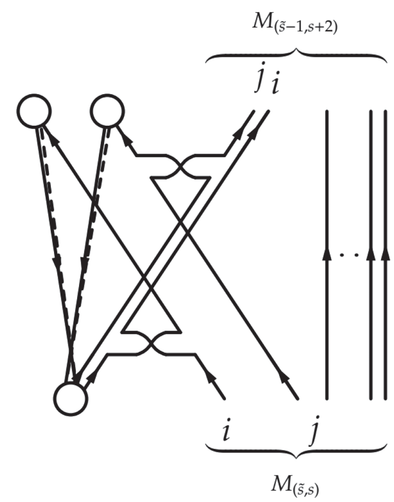

The amplitude is

$$\mathcal{M}_{(\tilde{s},s)\to(\tilde{s}+1,s-2)} \sim \frac{1}{N_c^2} \times \frac{1}{N_c^2} \times N_c^2 \times \tilde{s} = \frac{\tilde{s}}{N_c^2} \tag{56}$$

Maximally this process scales as $\sim \frac{1}{N_c}$, which is suppressed compared to the scaling of the mass of $M_{(\tilde{s},s)}$.

C. Flavor structure in the hadronic spectrum

So far, we have studied the composite spectrum of the theory without including the conjugated quarks $\bar{q}_{\dot{\alpha},i}, \bar{\tilde{q}}_{\dot{\alpha},[ij]}, \bar{Q}^{i,f}_{\dot{\alpha}}$. We will now, for the sake of completeness, consider broadly the spectrum, correlation functions and interactions when they are included.

Flavor in the chiral large N_c extension: The antifundamental quarks $Q_{i,f}$ have an $SU(N_c-3)$ flavor-index, while the fundamental quarks q^i, and two-index antisymmetric quarks $\tilde{q}^{[ij]}$ do not. How does this flavor-index contribute in interactions between hadrons? First, any intermediate state will be filled by gluons, two-index antisymmetric quarks $\tilde{q}$ and quarks with a flavor index Q_f, because they all have free energy scaling as $\sim N_c^2$. Second, the flavor index can form loops. Flavor loops can only be created by flavor-contracted operators such as $T_f{}^f = Q_{i,f}\tilde{q}^{[ij]}\bar{\tilde{q}}_{[jk]}\bar{Q}^{k,f}$. Third, operators can have free flavor indices, which do not alter the scaling of any given diagram.

When considering the full spectrum, there are groups of hadrons that have all gauge indices contracted in an identical manner, but for which their flavor indices differ (consider e.g., $X_f = q^i Q_{i,f}$ versus $X = q^i \bar{q}_i$). In this section we will divide the spectrum into composite operators that contain no Q_f quarks and all the remaining ones that contain at least one Q_f quark. The former set therefore contains no flavor indices (free or contracted) while the latter set contains at least one flavor index. In the case where the latter set contains multiple Q_f fields the flavor indices can be either free or contracted. The former set of composite operators that contains no Q_f quarks will be called flavorless operators while the latter set that contains at least one Q_f quark will be called flavored operators. Note that this distinction implies that the two flavor singlet operators $T = \bar{q}_i\tilde{q}^{[ij]}\bar{\tilde{q}}_{[jk]}q^k$ and $T_f{}^f = Q_{i,f}\tilde{q}^{[ij]}\bar{\tilde{q}}_{[jk]}\bar{Q}^{k,f}$ do not belong to the same group. According to our definition the former composite operator is flavorless while the latter is flavored. We will now study the interactions of the flavorless and flavored hadrons.

In the full spectrum, gauge singlet flavorless operators composed of n_q fields have multiple gauge singlet flavored analogs also composed of n_q fields. The spin may in general differ between the various operators. Consider as an example the following four-quark operator

$$T = q^i \bar{\tilde{q}}_{[ij]}\tilde{q}^{[jk]}\bar{q}_k \tag{57}$$

There exists three flavored four-quark analogs of this operator, one for each possible $q \to Q$ swap.

$$T_f = q^i \bar{\tilde{q}}_{[ij]}\tilde{q}^{[jk]}Q_{k,f}$$
$$T^f_{f'} = \bar{Q}^{i,f}\bar{\tilde{q}}_{[ij]}\tilde{q}^{[jk]}Q_{k,f'}$$

These three operators comprise the full set of four-quark gauge singlet flavored operators (without any gluon operators). Notice that the spin of the flavorless T and flavored operators $T_f, T^f_{f'}$ are typically not the same. Also note that the operator $T^f_{f'}$ decomposes into a flavor singlet T^f_f and flavor adjoint of the $SU(N_c-3)$ flavor group.

We can use three-point functions to highlight how diagrams with flavor-loops differ from diagrams without. Compare $\langle TTT\rangle$-diagrams with $\langle T^f_f T^{f'}_{f'} T^{f''}_{f''}\rangle$-diagrams

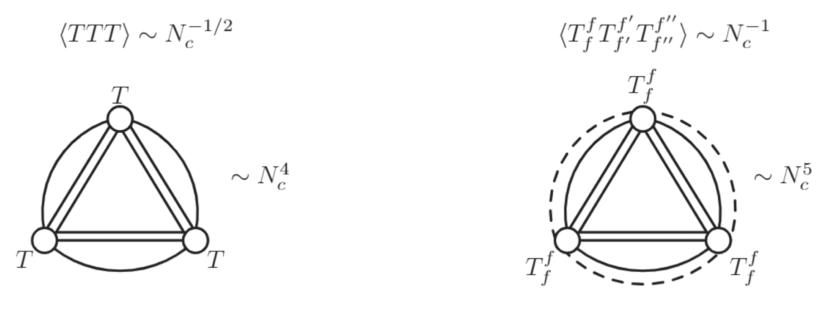

First the flavor-loop provides a factor of $\sim N_c$ to a diagram. Second any flavor-contracted operator like T^f_f will have a higher normalization factor by a factor of $\sqrt{N_c}$ compared to the flavorless analog T. In combination this yields an additional $N_c \times N_c^{-3/2} = 1/\sqrt{N_c}$ suppression of the second correlation function compared to the first.

Generally, any n-point function of T^f_f is $\sim N_c^{(2-n)/2}$ suppressed compared to an n-point function of T.

Consider now composite operators in which all gauge indices are contracted in a nontrivial way. In other words the composite operator is not composed of a product of gauge invariant operators. In addition we also take the operator to not have any gauge indices contracted by $\epsilon_{i_1\ldots i_{N_c}}$ of the gauge group $SU(N_c)$. This implies that the one-index quarks $q^i, Q_{i,f}$ and their conjugated $\bar{q}_i, \bar{Q}^{i,f}$ can appear at most twice in the operator. In addition to these restrictions, we will temporarily ignore operators composed entirely of two-index antisymmetric quarks $\tilde{q}$.

Flavorless hadrons: What is left of the hadron spectrum is quite limited. Before discussing their flavored analogs, we will first describe the flavorless hadrons with two one-index quarks. There are infinitely many of them, but they are easy to enumerate

$$\begin{aligned} X &= q^i \bar{q}_i \\ Y &= q^i q^j \bar{\tilde{q}}_{[ij]} \\ T &= q^i \bar{\tilde{q}}_{[ij]} \tilde{q}^{[jk]} \bar{q}_k \\ P &= q^i \bar{\tilde{q}}_{[ij]} \tilde{q}^{[jk]} \bar{\tilde{q}}_{[kl]} q^k \\ H &= q^i \bar{\tilde{q}}_{[ij]} \tilde{q}^{[jk]} \bar{\tilde{q}}_{[kl]} \tilde{q}^{[lh]} \bar{q}_h \\ &\dots \end{aligned} \tag{58}$$

Allowed n-point functions involving any combination of the above hadrons all scale exactly the same in N_c. The reason is as follows: In the leading order diagrams, there is one fundamental quark loop running on the boundary $\sim N_c$. Each operator insertion then creates $\tilde{s}$ additional color loops (one for each $\tilde{q}$) $\sim N_c^{\tilde{s}}$, implying a $N_c^{(1+2\tilde{s})/2}$ normalization factor. Thus, each operator gives a factor of $N_c^{\tilde{s}} \times N_c^{-(1+2\tilde{s})/2} = N_c^{-1/2}$. In total then, n-point functions with flavorless operators in Eq. (58) scale like $\sim N_c^1 (N_c^{-1/2})^n = N_c^{1-n/2}$.

Some n-point functions vanish. Two examples are $\langle YYY \rangle$ and $\langle PYX \rangle$. This is so since in general, a $\tilde{q}$-line started by one operator must be ended by another. Because of the color structure of the various quarks, this also enforces the restriction that fermionic operators cannot form odd n-point functions.

Motivated by the fact that all n-point functions scale exactly the same, we will now construct some simplified diagrams that will quickly visualize how the n-point functions of the above described hadrons are organized. Any three-point function is represented by a triangle. The lines of the triangle represent the quark loop and the three vertices represent the three operators. An example is

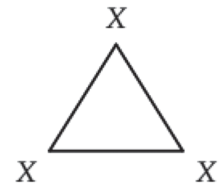

To keep track of the two-index antisymmetric quarks, each vertex additionally produces $\tilde{s}$ lines internally in the triangle

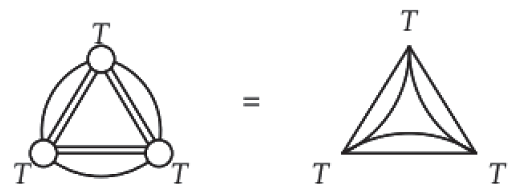

With this setup, all the three point functions with X, Y, T, P, H are

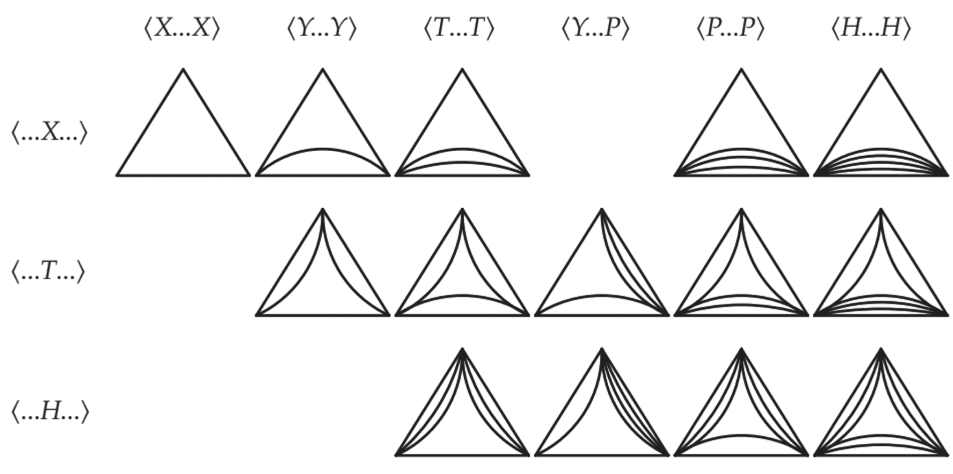

These all scale like $\sim N_c^{-1/2}$. Four-point functions are squares scaling like $\sim N_c^{-1}$, five-points are pentagons scaling like $\sim N_c^{-3/2}$ etc. At this point we have a solid handle on this group of flavorless operators. All their n-point functions scale the same, and we can quickly find out what n-point functions are allowed by gauge structure.

Flavored hadrons: For each of the above flavorless diagrams, there are a number of equivalent diagrams in the flavored sector—mixing flavorless operators with flavored ones, and flavored ones with other flavored ones. In our simplified diagrams, these can be created from, e.g., the flavorless triangles by replacing any of the solid outer lines with dashed flavor-lines (the dashed line is a shorthand for the $Q_{i,f}$ propagator). An example is the diagram for $\langle X_f X^f X \rangle$

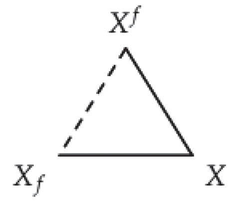

This allows us to quickly enumerate, for any three-point function of operators appearing in Eq. (58), *all* flavored analogs. Keep in mind that the inside of the diagram is irrelevant when comparing flavored diagrams to flavorless ones

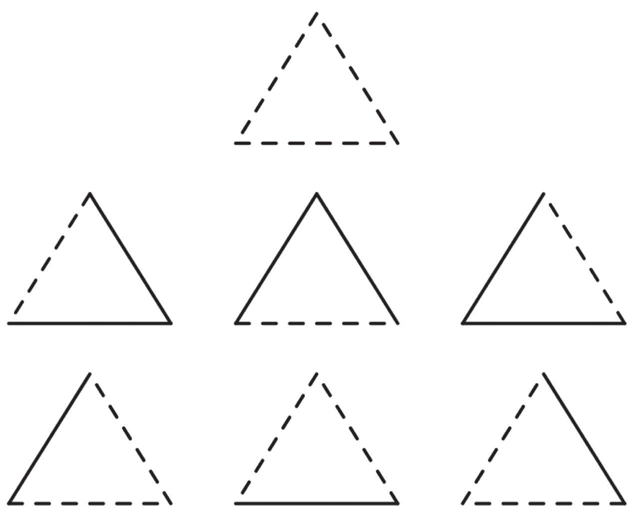

These diagrams tell us about how the flavorless sector interacts with the flavored sector. First, we see that the flavor-operators must appear in pairs or larger groups. Second, the scaling of a generic diagram is not altered by substitution of any number of the solid lines with dashed lines. However, if all n operators are flavor-contracted (like T^f_f), they form a flavor loop and the diagram is suppressed by a factor of $N_c^{(2-n)/2}$ as we noted earlier. Third, for flavorless three-point functions with *one* operator such as $\langle TTT \rangle$, there are three flavored analogs. For *two* different operators, fx. $\langle XYY \rangle$, there are five flavored analogs. For flavorless three-point functions with *three* different operators, fx. $\langle YTP \rangle$, all of the above seven triangles are unique flavored analogs of the flavorless triangle. This can be generalized to arbitrary n-point functions. In general, depending on how many different operators are involved, an n-point function will have between $n_- - 1$ and $n_+ - 1$ flavored analogs where

$$n_- = \begin{cases} \frac{2n^2+16}{8}, & n \text{ even} \\ \frac{2n^2+14}{8}, & n \text{ odd} \end{cases}, \qquad n_+ = 2^n \tag{59}$$

Hadrons made exclusively of two-index quarks: Now we come back to the operators made exclusively of two-index quarks. They are also easy to enumerate

$$\begin{aligned} L_2 &= \tilde{q}^{[ij]} \bar{\tilde{q}}_{[ji]} \\ L_4 &= \tilde{q}^{[ij]} \bar{\tilde{q}}_{[jk]} \tilde{q}^{[kl]} \bar{\tilde{q}}_{[li]} \\ L_6 &= \tilde{q}^{[ij]} \bar{\tilde{q}}_{[jk]} \tilde{q}^{[kl]} \bar{\tilde{q}}_{[lh]} \tilde{q}^{[hr]} \bar{\tilde{q}}_{[ri]} \\ &\dots \end{aligned}$$

In [62] the authors studied n-point functions of L_4 operators, so we will move forward and study n-point functions that combine L_{2i} operators with the $X, Y, T, P, H\dots$ operators. When combined with the $X, Y, T, P, H\dots$ operators the L_{2i}, $i \in \mathbb{Z}^{++}$ operators should be inserted inside the quark loop where the two-index quarks are. Each such insertion costs a factor of N_c^{-1} independent of i. This is because any L_{2i} insertion creates $i-1$ extra color loops, but also comes with a normalization factor of N_c^i. In terms of our simplified diagrams, we may add the L_{2i} operators as points that consume / produce $2i$ internal lines. An example is

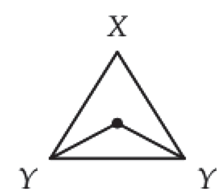

Again we can diagrammatically enumerate every possible n-point function. Using X, Y, T, all four-point functions with just one L_2 or L_4 or L_2 operator in the middle, are given by the diagrams

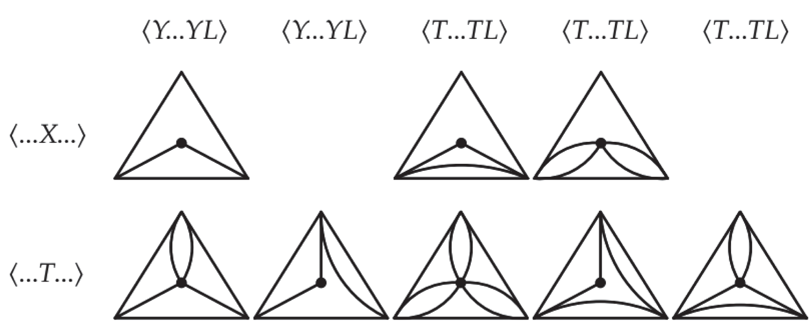

These all scale like $\sim N_c^{-3/2}$. What happens inside the triangles does not affect our flavor considerations—it is still true that any of the above diagrams have flavor-analogs that scale exactly the same.

Only the flavor-loops in the above analysis utilize the fact that f is a flavor-index with $\sim N_c$ flavors, and they end up being suppressed. Nevertheless, we have sketched a diagrammatic program for charting a subsection of the full hadronic spectrum, and shown that interactions between the flavorless and flavored sectors follow simple patterns. One-flavor index operators begin interacting with their flavorless analogs in three-point functions $\sim N_c^{-1/2}$. Two-flavor index operators begin interacting with their flavorless-analogs in four-point functions $\sim N_c^{-1}$. A notable exception to the suppression of mixing between the flavorless and flavored sectors are interactions such as $\langle X_f^f L_2\rangle \sim 1$.

VI. DISCUSSION

We set out to study QCD in a large N_c extension which is intermediate between the renowned 't Hooft and Orientifold extensions. Using standard large N_c techniques, we have systematically examined properties and interactions of multiple composites in the hadronic spectrum in the chiral extension of QCD.

First, we examined the purely left-handed and right-handed part of the hadronic spectrum. Here, $B, \tilde{B}$ and $M_{(1,N_c-2)}$ are the standard baryons and meson, while the rest ($\tilde{B}_{N_c/2}, \tilde{B}_{\text{even}}$, $\mathcal{B}_{f_1\ldots f_{N_c}}$, $M_{(\bar{s},s)}$, $X_f, Y_{ff'}$) all vanish at $N_c = 3$.

Using a diagrammatic analysis and group theoretical factors, we determined the N_c scaling of the different hadron masses to be proportional to the number of constituent quarks. Next, a study of simple gluon exchanges between hadrons showed that scattering amplitudes between hadrons follow a number-of-quarks and quark-type hierarchy: The hadrons with $n_q \sim N_c^2$ interact with all other hadrons, and are only scattered only by themselves. Hadrons with $n_q \sim N_c$ scatter with each other if they have a sufficient amount of quark content in common. Hadrons with $n_q \sim 1$ are scattered by higher $n_q \sim N_c$-hadrons if they have a sufficient number of quarks of the same type as the $n_q \sim 1$-hadron.

Only even n-point functions of X_f and $Y_{ff'}$ are nontrivial, and they are $N_c^{1+n/2}$ suppressed. However, X_f and $Y_{ff'}$ play crucial roles in other processes. They appear in the decay of two distinct baryonium states. The amplitude for such a decay depends on how many quarks are in the bound states, and ranges from $\sim N_c^0$ to $\sim N_c^{-1}$ for the first baryonium, and from N_c^{-1} to N_c^{-2} for the second baryonium. We also considered a nontrivial scattering process between $M_{(\bar{s},s)}$ and $Y_{ff'}$, and found it to be at least N_c^{-1} suppressed.

Finally we considered composites made of a mix of the left- and right-handed quarks. To break down the daunting task of analyzing the complete spectrum, we divided it into manageable groups. The hadron operators that do not make use of $\epsilon_{i_1\ldots i_{N_c}}$, and are composed of two fundamental flavorless quarks, and any number of two-index antisymmetric quarks, are particularly easy to understand. Correlation functions involving n_1 of these operators all scale like $\sim N_c^{(2-n_1)/2}$. Next, hadron operators that are composed of i pairs of two-index quarks are also easy to understand. Their n_2-point functions scale like $\sim N_c^{-n_2}$. Interactions between the two above mentioned groups of hadrons scale like $N_c^{(2-n_1-2n_2)/2}$. Next, by performing swaps of the type $q \to Q$, flavored analogs of the above mentioned operators can be created. When analyzing n-point functions involving a mix of flavorless and flavored operators, the flavorless ones must appear in pairs. This means that mixing of the flavored and flavorless sectors begin in three-point diagrams which are $N_c^{-1/2}$ suppressed. Generally, mixing diagrams obtained by this procedure to form n-point functions have the same scaling as the flavorless ones, so at $n \geq 3$, there are many diagrams mixing the flavorless and flavored sectors. In particular, for any n, there are $2^n - 2$ different diagrams mixing flavorless and flavored operators.

For possible future research directions we note that it would be interesting to study this chiral extension in a holographic setting. Holographic QCD has been under intense investigations in the last 20 years [28,63–67]. Holography can be used to study, among numerous other topics, chiral symmetry breaking [68], nuclear physics with a solitonic approach [69,70], and several additional topics using the Veneziano limit of QCD to construct holographic models (V-QCD) [22–25]. Quite recently QCD in the 't Hooft large N_c limit has also been under investigations using bootstrap techniques [71–73]. It would be highly interesting to do similar bootstrap studies of the chiral large N_c extension investigated here.

Furthermore, one can study angular-momentum contributions to the masses of the composites. Additionally, one can also study possible spin-flavor relations analogous to the ones derived in the 't Hooft limit, for the $N_c - 3$ antifundamental quarks. Some relevant literature can be found in [17–19,74].

In other words we believe our investigations open up for many new and exciting research projects.

APPENDIX: CANONICAL LAGRANGIAN

We now write down the canonically normalized Lagrangian of the theory in terms of the fields $A_\mu^a, q_\alpha^i, \tilde{q}_\alpha^r, Q_{\alpha,i,f}$

$$\mathcal{L} = -\frac{1}{4}F^a_{\mu\nu}F^{a,\mu\nu} + i\bar{q}_{\dot\alpha,i}\bar{\sigma}^{\mu,\dot\alpha\alpha}D^i_{\mu,j}q^j_\alpha + i\bar{\tilde{q}}^r_{\dot\alpha}\bar{\sigma}^{\mu,\dot\alpha\alpha}D^{rs}_\mu\tilde{q}^s_\alpha + i\bar{Q}^{i,f}_{\dot\alpha}\bar{\sigma}^{\mu,\dot\alpha\alpha}D_{\mu,i}{}^jQ_{\alpha,j,f} - \frac{1}{2\xi}(\partial^\mu A^a_\mu)^2 + \bar{c}^a(-\partial^\mu D^{ac}_\mu c^c) \tag{A1}$$

where

$$F^a_{\mu\nu} = \partial_\mu A^a_\nu - \partial_\nu A^a_\mu + gf^{abc}A^b_\mu A^c_\nu \tag{A2}$$

$$D^i_{\mu,j} = \partial_\mu \delta^i{}_j - igA^a_\mu (T^a_F)^i{}_j. \tag{A3}$$

$$D^{rs}_\mu = \partial_\mu\delta^{rs} - igA^a_\mu(T^a_{2A})^{rs} \tag{A4}$$

$$D_{\mu,i}{}^j = \partial_\mu\delta_i{}^j - igA^a_\mu(T^a_{\bar{F}})_i{}^j \tag{A5}$$

$$D^{ac}_\mu = \partial_\mu\delta^{ac} - igA^b_\mu(T^b_A)^{ac} \tag{A6}$$

The notation for Hermitian conjugation follows

$$(A^a_\mu)^\dagger = A^a_\mu, \qquad (q^i_\alpha)^\dagger \equiv \bar{q}_{\dot\alpha,i}, \qquad (\tilde{q}^r_\alpha)^\dagger \equiv \bar{\tilde{q}}^r_{\dot\alpha}, \qquad (Q_{\alpha,i,f})^\dagger \equiv \bar{Q}^{i,f}_{\dot\alpha}, \qquad (c^a)^\dagger = \bar{c}^a \tag{A7}$$

We have also chosen linear covariant gauge with gauge parameter ξ and c^a are ghost fields in the adjoint representation. The propagators are the usual ones

$$\begin{aligned}\langle A^a_\mu(x)A^b_\nu(y)\rangle &= \Delta_{\mu\nu}(x-y)\delta^{ab}\\ \langle q^i_\alpha(x)\bar{q}_{\dot\alpha,j}(y)\rangle &= S_{\alpha\dot\alpha}(x-y)\delta^i{}_j\\ \langle Q^r_\alpha(x)\bar{Q}^s_{\dot\alpha}(y)\rangle &= S_{\alpha\dot\alpha}(x-y)\delta^{rs}\\ \langle\tilde{q}_{\alpha,i,f}(x)\bar{Q}^{j,f'}_{\dot\alpha}(y)\rangle &= S_{\alpha\dot\alpha}(x-y)\delta_i{}^j\delta_f{}^{f'}\\ \langle c^a(x)\bar{c}^b(y)\rangle &= \Delta(x-y)\delta^{ab}\end{aligned} \tag{A8}$$

We now switch to tensor notation for the gauge fields and $\tilde{q}$ Weyl fermions

$$A_\mu = A^a_\mu T^a_F, \qquad \tilde{q} = \tilde{q}^r A^r, \qquad c = c^a T^a_F \tag{A9}$$

and rescale the fields appropriately

$$A_\mu \to \frac{1}{g}A_\mu, \qquad q_\alpha \to \frac{1}{g}q_\alpha, \qquad \tilde{q}_\alpha \to \frac{1}{g}\tilde{q}_\alpha, \qquad Q_\alpha \to \frac{1}{g}Q_\alpha, \qquad c \to \frac{1}{g}c \tag{A10}$$

With these two changes we can write the Lagrangian as

$$\mathcal{L} = \frac{N_c}{\lambda}\Big[-\frac{1}{2}\mathrm{Tr}F_{\mu\nu}F^{\mu\nu} + i\bar{q}\bar{\sigma}^\mu D_\mu q + 2i\mathrm{Tr}(\bar{\tilde{q}}\bar{\sigma}^\mu D_\mu\tilde{q}) + i\bar{Q}\bar{\sigma}^\mu D_\mu Q - \frac{1}{\xi}\mathrm{Tr}(\partial^\mu A_\mu)^2 + 2\mathrm{Tr}\bar{c}(-\partial^\mu D_\mu c)\Big] \tag{A11}$$

with

$$F_{\mu\nu} = F^a_{\mu\nu}T^a_F = \partial_\mu A_\nu - \partial_\nu A_\mu - i[A_\mu, A_\nu] \tag{A12}$$

$$D_\mu q^i = \partial_\mu q^i - i(A_\mu)^i{}_j q^j, \qquad (A_\mu)^i{}_j = A^a_\mu(T^a_F)^i{}_j \tag{A13}$$

$$(D_\mu\tilde{q})^{ij} = \partial_\mu\tilde{q}^{ij} - i((A_\mu)^i{}_k\tilde{q}^{kj} + \tilde{q}^{ik}(A^T_\mu)_k{}^j), \qquad (A_\mu)^i{}_j = A^a_\mu(T^a_F)^i{}_j \tag{A14}$$

$$D_\mu Q_i = \partial_\mu Q_i - i(A_\mu)_i{}^j Q_j, \qquad (A_\mu)_i{}^j = A^a_\mu(T^a_{\bar{F}})_i{}^j = -A^a_\mu(T^{a,T}_F)_i{}^j \tag{A15}$$

$$(D_\mu c)^i{}_j = \partial_\mu c^i{}_j - i[A_\mu, c]^i{}_j, \qquad (A_\mu)^i{}_j = A^a_\mu(T^a_F)^i{}_j, \qquad (c)^i{}_j = c^a(T^a_F)^i{}_j \tag{A16}$$

and the 't Hooft coupling being $\lambda = g^2N_c$ and the gauge field is $A_\mu = A^a_\mu T^a_F$ for an appropriate representation r.

[1] D. J. Gross and F. Wilczek, Ultraviolet behavior of non-Abelian gauge theories, Phys. Rev. Lett. **30**, 1343 (1973).
[2] H. D. Politzer, Reliable perturbative results for strong interactions?, Phys. Rev. Lett. **30**, 1346 (1973).
[3] D. J. Gross and F. Wilczek, Asymptotically free gauge theories—I, Phys. Rev. D **8**, 3633 (1973).
[4] D. J. Gross and F. Wilczek, Asymptotically free gauge theories. 2., Phys. Rev. D **9**, 980 (1974).
[5] K. G. Wilson, Confinement of quarks, Phys. Rev. D **10**, 2445 (1974).
[6] M. Creutz, Monte Carlo study of quantized SU(2) gauge theory, Phys. Rev. D **21**, 2308 (1980).
[7] P. A. Baikov, K. G. Chetyrkin, and J. H. Kühn, Five-loop running of the QCD coupling constant, Phys. Rev. Lett. **118**, 082002 (2017).
[8] F. Herzog, B. Ruijl, T. Ueda, J. A. M. Vermaseren, and A. Vogt, The five-loop beta function of Yang-Mills theory with fermions, J. High Energy Phys. 02 (2017) 090.
[9] G. 't Hooft, A planar diagram theory for strong interactions, Nucl. Phys. **B72**, 461 (1974).

[10] E. Witten, Baryons in the 1/n expansion, Nucl. Phys. **B160**, 57 (1979).

[11] S. J. Brodsky, H.-C. Pauli, and S. S. Pinsky, Quantum chromodynamics and other field theories on the light cone, Phys. Rep. **301**, 299 (1998).

[12] S. J. Brodsky, G. F. de Teramond, H. G. Dosch, and J. Erlich, Light-front holographic QCD and emerging confinement, Phys. Rep. **584**, 1 (2015).

[13] F. Gross *et al.*, 50 years of quantum chromodynamics: Introduction and review, Eur. Phys. J. C **83**, 1125 (2023).

[14] P. Achenbach *et al.*, The present and future of QCD, Nucl. Phys. **A1047**, 122874 (2024).

[15] F. Sannino, Two-index SU(N) theories: QCD, orientifolds, super Yang-Mills, lattice and Steven Weinberg's $\pi\pi$ scattering legacy, arXiv:2402.05850.

[16] T. D. Cohen and R. F. Lebed, Are there tetraquarks at large N_c in QCD(F)?, Phys. Rev. D **90**, 016001 (2014).

[17] R. Dashen, E. Jenkins, and A. V. Manohar, Erratum: $\frac{1}{N_c}$ expansion for baryons, Phys. Rev. D **51**, 2489(E) (1995).

[18] E. Jenkins and R. F. Lebed, Baryon mass splittings in the $1/n_c$ expansion, Phys. Rev. D **52**, 282 (1995).

[19] R. F. Dashen, E. Jenkins, and A. V. Manohar, Spin-flavor structure of large N baryons, Phys. Rev. D **51**, 3697 (1995).

[20] G. Veneziano, Some aspects of a unified approach to gauge, dual and Gribov theories, Nucl. Phys. **B117**, 519 (1976).

[21] M. A. Luty, Baryons with many colors and flavors, Phys. Rev. D **51**, 2322 (1995).

[22] M. Jarvinen, Massive holographic QCD in the Veneziano limit, J. High Energy Phys. 07 (2015) 033.

[23] M. Jarvinen and E. Kiritsis, Holographic models for QCD in the Veneziano limit, J. High Energy Phys. 03 (2012) 002.

[24] T. Alho, M. Järvinen, K. Kajantie, E. Kiritsis, C. Rosen, and K. Tuominen, A holographic model for QCD in the Veneziano limit at finite temperature and density, J. High Energy Phys. 04 (2014) 124; 02 (2015) 033(E).

[25] T. Alho, M. Järvinen, K. Kajantie, E. Kiritsis, and K. Tuominen, On finite-temperature holographic QCD in the Veneziano limit, J. High Energy Phys. 01 (2013) 093.

[26] E. Corrigan and P. Ramond, A note on the quark content of large color groups, Phys. Lett. **87B**, 73 (1979).

[27] E. B. Kiritsis and J. Papavassiliou, An alternative large N limit for QCD and its implications for low-energy nuclear phenomena, Phys. Rev. D **42**, 4238 (1990).

[28] C. Hoyos and A. Karch, Alternative large n baryons and holography, Phys. Rev. D **79**, 125021 (2009).

[29] A. Armoni, G. Shore, and G. Veneziano, Quark condensate in massless QCD from planar equivalence, Nucl. Phys. **B740**, 23 (2006).

[30] A. Armoni and A. Patella, Degeneracy between the regge slope of mesons and baryons from supersymmetry, J. High Energy Phys. 07 (2009) 073.

[31] S. Bolognesi, Baryons and Skyrmions in QCD with quarks in higher representations, Phys. Rev. D **75**, 065030 (2007).

[32] A. Cherman and T. D. Cohen, The Skyrmion strikes back: Baryons and a new large N_c limit, J. High Energy Phys. 12 (2006) 035.

[33] A. Cherman, T. D. Cohen, and R. F. Lebed, All you need is N: Baryon spectroscopy in two large N limits, Phys. Rev. D **80**, 036002 (2009).

[34] A. Cherman and T. D. Cohen, A tale of two Skyrmions: The nucleon's strange quark content in different large n limits, Phys. Lett. B **641**, 401 (2006).

[35] A. Armoni, M. Shifman, and G. Veneziano, Exact results in nonsupersymmetric large N orientifold field theories, Nucl. Phys. **B667**, 170 (2003).

[36] A. Armoni, M. Shifman, and G. Veneziano, SUSY relics in one flavor QCD from a new 1/N expansion, Phys. Rev. Lett. **91**, 191601 (2003).

[37] A. Armoni, M. Shifman, and G. Veneziano, QCD quark condensate from SUSY and the orientifold large N expansion, Phys. Lett. B **579**, 384 (2004).

[38] A. Armoni, M. Shifman, and G. Veneziano, From super Yang-Mills theory to QCD: Planar equivalence and its implications, in *From Fields to Strings: Circumnavigating Theoretical Physics. Ian Kogan Memorial Collection (3 volume set)*, edited by M. Shifman, A. Vainshtein, and J. Wheater (World scientific, 2004), pp. 353–444, 10.1142/9789812775344_0013.

[39] A. Armoni, M. Shifman, and G. Veneziano, Refining the proof of planar equivalence, Phys. Rev. D **71**, 045015 (2005).

[40] T. A. Ryttov and F. Sannino, Hidden QCD in chiral gauge theories, Phys. Rev. D **73**, 016002 (2006).

[41] H. Georgi, A tool kit for builders of composite models, Nucl. Phys. **B266**, 274 (1986).

[42] T. Appelquist, Z.-y. Duan, and F. Sannino, Phases of chiral gauge theories, Phys. Rev. D **61**, 125009 (2000).

[43] T. Appelquist, A. G. Cohen, M. Schmaltz, and R. Shrock, New constraints on chiral gauge theories, Phys. Lett. B **459**, 235 (1999).

[44] T. Appelquist and R. Shrock, Ultraviolet to infrared evolution of chiral gauge theories, Phys. Rev. D **88**, 105012 (2013).

[45] A. Armoni and M. Shifman, A chiral SU(N) gauge theory planar equivalent to super-Yang-Mills, Phys. Rev. D **85**, 105003 (2012).

[46] Y.-L. Shi and R. Shrock, Renormalization-group evolution of chiral gauge theories, Phys. Rev. D **91**, 045004 (2015).

[47] Y.-L. Shi and R. Shrock, $A_k\bar{F}$ chiral gauge theories, Phys. Rev. D **92**, 105032 (2015).

[48] Y.-L. Shi and R. Shrock, Dynamical symmetry breaking in chiral gauge theories with direct-product gauge groups, Phys. Rev. D **94**, 065001 (2016).

[49] S. Bolognesi, K. Konishi, and M. Shifman, Patterns of symmetry breaking in chiral QCD, Phys. Rev. D **97**, 094007 (2018).

[50] S. Bolognesi and K. Konishi, Dynamics and symmetries in chiral $SU(N)$ gauge theories, Phys. Rev. D **100**, 114008 (2019).

[51] S. Bolognesi, K. Konishi, and A. Luzio, Dynamics from symmetries in chiral $SU(N)$ gauge theories, J. High Energy Phys. 09 (2020) 001.

[52] S. Bolognesi, K. Konishi, and A. Luzio, Probing the dynamics of chiral $SU(N)$ gauge theories via generalized anomalies, Phys. Rev. D **103**, 094016 (2021).

[53] P. B. Smith, A. Karasik, N. Lohitsiri, and D. Tong, On discrete anomalies in chiral gauge theories, J. High Energy Phys. 01 (2022) 112.

[54] A. Karasik, K. Önder, and D. Tong, Chiral gauge dynamics: Candidates for non-supersymmetric dualities, J. High Energy Phys. 11 (2022) 122.
[55] M. M. Anber and S. Y. L. Chan, 2-index chiral gauge theories, J. High Energy Phys. 10 (2023) 025.
[56] P. Cvitanovic, *Group Theory: Birdtracks, Lie's, and Exceptional Groups* (Princeton University Press, Princeton, NJ, 2020).
[57] H. Georgi, *Lie Algebras In Particle Physics: From Isospin To Unified Theories* (Taylor & Francis, Boca Raton, 2000).
[58] A. V. Manohar, Large N QCD, in *Les Houches Summer School in Theoretical Physics, Session 68: Probing the Standard Model of Particle Interactions* (1998), pp. 1091–1169, arXiv:hep-ph/9802419.
[59] T. D. Cohen, D. L. Shafer, and R. F. Lebed, Baryons in $\mathrm{QCD}_{\mathrm{AS}}$ at large N_c: A roundabout approach, Phys. Rev. D **81**, 036006 (2010).
[60] F. Buisseret and C. Semay, Light baryon masses in different large-N_c limits, Phys. Rev. D **82**, 056008 (2010).
[61] C. Liu, Baryonium, tetra-quark state and glue-ball in large N_c QCD, Eur. Phys. J. C **53**, 413 (2008).
[62] T. D. Cohen and R. F. Lebed, Tetraquarks with exotic flavor quantum numbers at large N_c in QCD(AS), Phys. Rev. D **89**, 054018 (2014).
[63] N. Evans and A. Tedder, Perfecting the ultra-violet of holographic descriptions of QCD, Phys. Lett. B **642**, 546 (2006).
[64] N. Evans, Holography of strongly coupled gauge theories, EPJ Web Conf. **258**, 08001 (2022).
[65] R. Abt, J. Erdmenger, N. Evans, and K. S. Rigatos, Light composite fermions from holography, J. High Energy Phys. 11 (2019) 160.
[66] U. Gursoy and E. Kiritsis, Exploring improved holographic theories for QCD: Part I, J. High Energy Phys. 02 (2008) 032.
[67] U. Gursoy, E. Kiritsis, and F. Nitti, Exploring improved holographic theories for QCD: Part II, J. High Energy Phys. 02 (2008) 019.
[68] A. Gorsky, S. B. Gudnason, and A. Krikun, Baryon and chiral symmetry breaking in holographic QCD, Phys. Rev. D **91**, 126008 (2015).
[69] S. Baldino, S. Bolognesi, S. B. Gudnason, and D. Koksal, Solitonic approach to holographic nuclear physics, Phys. Rev. D **96**, 034008 (2017).
[70] S. Baldino, L. Bartolini, S. Bolognesi, and S. B. Gudnason, Holographic nuclear physics with massive quarks, Phys. Rev. D **103**, 126015 (2021).
[71] J. Albert and L. Rastelli, Bootstrapping pions at large N, J. High Energy Phys. 08 (2022) 151.
[72] J. Albert and L. Rastelli, Bootstrapping pions at large N. Part II: Background gauge fields and the chiral anomaly, arXiv:2307.01246.
[73] J. Albert, J. Henriksson, L. Rastelli, and A. Vichi, Bootstrapping mesons at large N: Regge trajectory from spin-two maximization, arXiv:2312.15013.
[74] F. Buisseret, N. Matagne, and C. Semay, Spin contribution to light baryons in different large-N limits, Phys. Rev. D **85**, 036010 (2012).